Clathrin-mediated Endocytosis Facilitates Internalization of *Magnaporthe oryzae* Effectors into Rice Cells

Ely Oliveira-Garcia[1,2]*, Tej Man Tamang[1,3], Jungeun Park[3], Melinda Dalby[1], Magdalena Martin-Urdiroz[4], Clara Rodriguez Herrero[4,5], An Hong Vu[2], Sunghun Park[3], Nicholas J. Talbot[5] & Barbara Valent[1]*

[1]Department of Plant Pathology, Kansas State University, Manhattan, KS 66506, U.S.A.

[2]Department of Plant Pathology and Crop Physiology, Louisiana State University, Baton Rouge, LA 70803, U.S.A.

[3]Department of Horticulture and Natural Resources, Kansas State University, Manhattan, KS 66506, U.S.A.

[4]School of Biosciences, University of Exeter, Exeter, EX4 4QD, UK

[5]The Sainsbury Laboratory, Norwich Research Park, Norwich NR4 7UH, UK.

*Corresponding authors: E. Oliveira-Garcia; E-mail: EOliveiraGarcia@agcenter.lsu.edu and B. Valent; E-mail: bvalent@ksu.edu

Short Title: Blast Effector Translocation By Endocytosis

* The author(s) responsible for distribution of materials integral to the findings presented in this article in accordance with the policy described in the Instructions for Authors (https://academic.oup.com/plcell/pages/General-Instructions) are: E. Oliveira-Garcia (EOliveiraGarcia@agcenter.lsu.edu) and B. Valent (bvalent@ksu.edu).

ABSTRACT

Many filamentous eukaryotic plant pathogens, such as fungi and oomycetes, deliver effectors into living plant cells to suppress defenses and control plant processes needed for infection. Little is known about the mechanism by which these pathogens translocate effector proteins across the plasma membrane into the plant cytoplasm. The blast fungus *Magnaporthe oryzae* secretes cytoplasmic effectors into a specialized biotrophic interfacial complex (BIC) before translocation. Here we show that cytoplasmic effectors within BICs are packaged into dynamic vesicles that can occasionally be found separated from BICs in the host cytoplasm. Live cell imaging with fluorescently-labelled rice lines showed that BICs are enriched in plant plasma membrane, actin, and Clathrin Light Chain-1, a marker for clathrin-mediated endocytosis (CME). We report that a novel cytoplasmic effector, Bas83, labels empty membrane vesicles surrounding BICs. Inhibition of CME using VIGS and chemical treatments results in a distinctive swollen BIC phenotype lacking effector vesicles. In contrast, fluorescent marker co-localization, VIGS and chemical inhibitor studies failed to support a major role for clathrin-independent endocytosis in effector vesicle formation. Taken together, this study provides evidence that cytoplasmic effector translocation is mediated by clathrin-mediated endocytosis in BICs and suggests a role for *M. oryzae* effectors in co-opting plant endocytosis.

INTRODUCTION

Many fungal and oomycete pathogens cause plant disease by hijacking and feeding on living plant cells, and they deliver effectors into and around host cells to promote infection (Giraldo and Valent, 2013; Lo Presti and Kahmann, 2017). This includes the Ascomycete fungus *Magnaporthe oryzae* (synonym of *Pyricularia oryzae*), which threatens global food security by causing blast diseases on rice, on several millets, and most recently on wheat (Gladieux et al., 2018; Valent et al., 2020). *M. oryzae* executes a hemibiotrophic lifestyle involving biotrophic invasion of successive plant cells by specialized intracellular invasive hyphae (IH) that grow from cell to cell (Kankanala et al., 2007). Blast IH growing in living host cells are enclosed by extensions of the plant plasma membrane termed the extra-invasive hyphal membrane (EIHM). Colonized cells die as they fill with hyphae and the EIHM and host vacuolar membranes become disrupted, while the fungus moves on to colonize neighboring cells using the same strategy (Kankanala et al., 2007; Mochizuki et al., 2015; Sakulkoo et al., 2018; Jones et al., 2021). Each successful IH undergoes

hyphal morphogenesis and is associated with differentiated interfacial zones after entering the host cell lumen (Kankanala et al., 2007; Khang et al., 2010). Specifically, appressorial penetration pegs enlarge into tubular filamentous hyphae, called primary invasive hyphae, which are enclosed in EIHM with an extended dome-shaped cap, the Biotrophic Interfacial Complex (BIC). BICs accumulate cytoplasmic effectors destined for translocation into the host cytoplasm. Tubular primary hyphae then transition to a bulbous pseudohyphal-like growth form. BICs at the tips of primary hyphae are left behind beside the first bulbous IH cell during the differentiation process, and they continue to accumulate cytoplasmic effectors as the bulbous IH grow to fill the cell (Khang et al., 2010). Mutation in an effector gene, Required-for-Focal-BIC-Formation 1 (*RBF1*), encoding a glycine-rich secreted protein, results in dispersed cytoplasmic effector localization around BIC-associated cells (the primary hyphae and first bulbous IH cell), perturbs primary hyphal structure, and decreases pathogenicity (Nishimura et al., 2016; Nishizawa et al., 2016).

In blast disease, cytoplasmic and apoplastic effectors are clearly differentiated by the fungal secretion system used and their localization pattern after secretion. Primary hyphae and the first bulbous IH focally secrete cytoplasmic effectors into BICs using a specialized, Golgi-independent secretion system. In *M. oryzae*, and also in the oomycete potato pathogen *Phytophthora infestans*, secretion of cytoplasmic effectors differs from secretion of apoplastic effectors in being insensitive to treatment with Brefeldin A (BFA), a chemical known to inhibit conventional Golgi-mediated secretion in fungi (Giraldo et al., 2013; Van den Ackerveken, 2017; Wang et al., 2017). Fluorescent cytoplasmic effectors are routinely detected in the cytoplasm of invaded cells, and some are also detected in the cytoplasm of surrounding uninvaded host cells, apparently moving through plasmodesmata to prepare neighboring cells before invasion (Khang et al., 2010). In contrast, apoplastic effectors, such as the biotrophy-associated secreted protein 4 (Bas4), the LysM protein 1 (Slp1), and Bas113, are secreted via conventional golgi-mediated secretion, and they accumulate uniformly throughout the apoplastic compartment enclosed within the EIHM, outlining the entire IH without bleeding into the plant cell wall (Mosquera et al., 2009; Mentlak et al., 2012; Giraldo et al., 2013). Indeed, localization of secreted Bas4 fluorescent fusion proteins has become a reliable live cell imaging marker for the intactness of the EIHM around IH (Khang et al., 2010; Mochizuki et al., 2015; Jones et al., 2021). After filling the host cell, hyphal differentiation and BIC relocalization recur for each new hypha that enters a living neighbor cell (Khang et al., 2010; Sakulkoo et al., 2018).

The mechanism by which eukaryotic filamentous plant pathogens deliver effectors across the host plasma membrane inside living host cells is poorly understood and the mechanism is likely to vary in different systems (Giraldo and Valent, 2013; Petre and Kamoun, 2014; Fawke et al., 2015; Lo Presti et al., 2015; Lo Presti and Kahmann, 2017). Amino acid translocation motifs have been identified for oomycete effectors, with the RXLR motif being the most common, although cell entry motifs for fungal effectors have not been defined. The RXLR motif in oomycete effectors was reported to mediate host cell uptake through endocytosis based on binding to phosphatidylinositol-3-phosphate (PI3P) in host membrane (Kale et al., 2010), although it was recently shown that the RXLR motif from *Phytophthora infestans* effector AVR3a is cleaved off before secretion from the pathogen (Wawra et al., 2017). Therefore, the function of RXLR motif in cell entry remains disputed (Petre and Kamoun, 2014; Trusch et al., 2018). Another amino acid motif, YKARK, appears involved in translocation of the effector SpHtp3 from *Saprolegnia parasitica*, a serious oomycete pathogen of fish, inside fish cells (Trusch et al., 2018). Specifically, this effector appears to be internalized inside host cells via lipid-raft mediated endocytosis through binding to a gp96-like receptor, and another effector is involved in releasing SpHtp3 from vesicles into the fish cytoplasm. In an example from a fungal pathogen, a solvent-exposed RGD vitronectin-like motif is required for internalization of ToxA, a host-specific proteinaceous toxin secreted by the necrotrophic wheat pathogen *Pyrenophora tritici-repentis* (Manning and Ciuffetti, 2005). In addition to uptake by plant endocytosis, effectors might enter plant cells through specialized translocon complexes in the plasma membrane. For example, the human malaria parasite, *Plasmodium falciparum*, is contained within a parasitophorous vacuole inside invaded red blood cells, and effectors are delivered across the membrane into the host cytoplasm by the PTEX translocon (Elsworth et al., 2014). Recently, a stable protein complex comprised of five unrelated fungal effectors and two fungal membrane proteins has been implicated in effector translocation by the maize smut fungus *Ustilago maydis* (Ludwig et al., 2021). However, the question of how effectors are taken up into plant cells remains largely unresolved for eukaryotic plant pathogens.

Clathrin-mediated endocytosis (CME) is the major mechanism by which eukaryotic cells internalize extracellular or membrane-bound cargoes, and this process is best understood in mammalian systems and yeast (Kaksonen and Roux, 2018). Increasing understanding of CME in plants shows both conserved and evolutionarily unique mechanistic details (Qi et al., 2018;

Reynolds et al., 2018; Johnson et al., 2020; Narasimhan et al., 2020). CME is known to play key roles in plant-microbe interactions (Dodds and Rathjen, 2010; Beck et al., 2012; Fan et al., 2015). CME is required for immunity mediated by pattern recognition receptor kinases, for instance, specifically through internalization of activated extracellular pattern recognition receptors (PRRs) for degradation in the vacuole (Mbengue et al., 2016). Examples include the pattern recognition receptor Pep receptor 1/2 (PEPR1/2), the EF-TU receptor (EFR) recognizing the PAMP bacterial elongation factor, and FLS2 recognizing the PAMP flagellin (flg-22) (Spallek et al., 2013; Mbengue et al., 2016), as well as the Cf-4 receptor-like protein that recognizes the *C. fulvum* Avr4 avirulence effector (Postma et al., 2016). Trafficking of activated PRRs requires clathrin and converges onto endosomal vesicles that are also shared by the hormone receptor Brassinosteriod Insensitive 1 (BRI1). Additionally, it is known that pathogens can control plant CME. In addition to its role in suppressing INF1-mediated cell death, the *P. infestans* host-translocated RXLR effector AVR3a was recently shown to associate with the Dynamin-Related Protein 2, a plant GTPase implicated in receptor-mediated endocytosis, and to suppress flg22-triggered defense responses and reduce FLS2 internalization (Chaparro-Garcia et al., 2015). Therefore, AVR3a interacts with a membrane-remodeling complex involved in immune receptor-mediated endocytosis. Also, in host cells containing haustoria from the oomycete *P. infestans*, the late endosomal pathway is rerouted from the vacuole to the extrahaustorial membrane (EHM) surrounding haustoria (Bozkurt et al., 2015). Multiple effectors from this pathogen are now implicated in rerouting the host membrane trafficking system and autophagy machinery for the benefit of the invading pathogen (Bozkurt et al., 2015; Dagdas et al., 2018; Petre et al., 2021).

Effector translocation in the *M. oryzae*/rice pathosystem can be assayed directly by live cell imaging of fluorescently-labeled effector proteins inside host cells after secretion by IH invading rice leaf sheath cells (Khang et al., 2010). Although some effectors naturally localize to host nuclei, addition of a nuclear localization signal (NLS) to fluorescent effectors enhances visualization of translocation and cell-to-cell movement. Blast cytoplasmic effectors apparently do not contain a translocation motif as reported for oomycete effectors. Instead, preferential accumulation in the BIC, which is a prominent feature of the *M. oryzae*-rice cell interface, is the major predictor for translocation into the rice cell. Previously, Nishizawa and colleagues reported that a cytoplasmic effector occurs in vesicles in an outer BIC region (Mochizuki et al., 2015; Nishimura et al., 2016; Nishizawa et al., 2016). Here, we have used live-cell fluorescence imaging

to characterize the nature and dynamics of membrane-bound effector vesicles within BICs and in surrounding host cytoplasm. We show that BICs are enriched for CME components, and we report functional analyses using virus-induced gene silencing (VIGS) and pharmacological approaches. When considered together, our data indicate that blast effectors are internalized through clathrin-mediated endocytosis in the outer BIC layers, followed by escape from the vesicles into the rice cytoplasm.

RESULTS

BICs contain multiple vesicles labeled by cytoplasmic effectors

BICs were previously reported as interfacial structures containing fluorescently-labelled apoplastic effectors, such as Bas4:eGFP, in an inner base layer and a concentration of fluorescent cytoplasmic effectors in the outer 'dome-shaped' region (Khang et al., 2010; Nishizawa et al., 2016). We now routinely resolve the dome region of BICs by laser confocal imaging as a concentration of vesicles containing fluorescent cytoplasmic effectors (Figure 1). These effector vesicles are illustrated by an image of a BIC at the tip of a primary hypha (tip-BIC) expressing fluorescent apoplastic effector Bas4:eGFP and fluorescent cytoplasmic effector Pwl2:mRFP (Figure 1A). The Bas4:eGFP fluorescence remains evenly distributed throughout the EIHM matrix around the growing IH, including in an inner layer of the BIC. In contrast, Pwl2:mRFP occurs as distinct vesicles in the outer BIC region. We have observed effector vesicles in tip-BICs labeled with additional translocated effectors Bas1 and Pwl1 fused to either eGFP or mRFP (Supplemental Figure S1). Vesicles are also observed after tip-BICs move beside the first bulbous IH cells (side-BICs) (Figure 1B; Figure S2). We evaluated the proximity of these vesicles relative to both tip- and side-BICs. Whereas the vast majority of vesicles associated with primary IH were located in the tip-BIC, some vesicles associated with side-BICs were found in regions of the cytoplasm at least 7 µm from the fungal cell wall at the BIC, which we define as outside the BIC (Figure 1C). Inclusion of the apoplastic effector Bas4:eGFP in these experiments confirmed that the EIHM remained intact at each infection site, based on its uniform outlining of the IH and lack of spilling into the invaded rice cell.

We identified a novel cytoplasmic effector, Bas170 (MGG_07348.6), that localized in vesicles in the rice cytoplasm short distances from the appressorial penetration site at a stage before primary hyphal growth is visible. The Bas170:mRFP fusion protein naturally accumulates in the

rice nucleus at this very early infection stage, presumably to reprogram plant transcription essential for *M. oryzae* infection (Figure 1D). These results suggest rapid effector translocation from appressoria even before growth of primary IH. Bas170:mRFP also labels BIC-associated vesicles in tip-BICs and side BICs after growth of IH in the cell (Figure 1E,F). Vesicles observed using fluorescent Bas170 fusion proteins are similar to vesicles observed with Pwl2, Pwl1 and Bas1 fusion proteins except that these latter effectors were not observed under appressoria at the earlier time period.

Vesicles in BICs are dynamic through time

To understand vesicle dynamics in BICs through time, we imaged BIC effector fluorescence during the morphogenic switch from tubular primary hyphae to bulbous IH using a strain co-expressing two cytoplasmic effectors, Bas1:eYFP and Pwl2:mRFP (Figure 2). The vesicle content varied over the 2-hour period when the tip-BIC was displaced from the primary hyphal tip to the side-BIC beside the differentiating bulbous IH cell. Tip-BICs often contained vesicles with either red or green fluorescence, rather than yellow expected for co-localization, suggesting that effectors can be sorted into different vesicles. For this series of experiments, Pwl2:mRFP occurred in vesicles that reached outer layers of the tip-BIC compared to Bas1:eYFP. Pwl2:mRFP appeared less abundant relative to Bas1:eYFP during the switch from tip- to side-BIC, recovering again after growth of bulbous IH (Figure 2A). Both vesicle size and content varies within BICs through time (Figure 2 B-F). Specifically, BICs at primary hyphal tips contain a larger number of smaller vesicles (Figure 2D,E). Whereas BICs on primary hyphae deliver effectors in ‘micro-vesicles’ ranging from 41 nm to 114 nm, BICs on mature bulbous hypha contain effectors in ‘macro-vesicles’ ranging from 153 nm up to 2310 nm at times (Figure 2C,D). Effector vesicles beside mature bulbous IH often showed colocalization of fluorescence from different effectors compared to vesicles in tip-BICs (Figure 2A, B and F).

Cytoplasmic connections were observed between BICs and plant cytoplasm at the periphery of the invaded cell, illustrated in optical sections through a BIC in Supplemental Movie S1. This is consistent with a previous report of dynamic connections linking BICs and host cytoplasm underneath the appressorium (Khang et al., 2010). These cytoplasmic connections may facilitate movement of effectors from cytoplasm surrounding the BIC in the cell center to the peripheral cytoplasm, in position to rapidly move through plasmodesmata into neighboring cells.

BIC vesicles contain plant plasma membrane

Effector-labeled vesicles in the BIC could arise through secretion of cytoplasmic effectors in fungal exosomes or through plant endocytosis. We previously reported that BICs are enriched in plant plasma membrane based on infection of transgenic rice expressing a plasma membrane marker (Giraldo et al., 2013). Here we again use LTi6B:GFP-labeled rice to confirm that BICs contain abundant plant plasma membrane (Figure 3A,B). Individual effector vesicles were observed to be surrounded by labeled plant plasma membrane (Figure 3C), especially for vesicles in side-BICs on mature bulbous hyphae, where the vesicles reach diameters of 150 nm or larger.

To further confirm that BIC vesicles contain plant plasma membrane, we evaluated BIC membrane composition by staining with the endocytosis tracker dyes FM 4-64 and FM 1-4 (Figure 3D,E). These amphiphilic styryl dyes insert in the plasma membrane where they diffuse laterally in the membrane and are only internalized into the cell via endocytosis (Atkinson et al., 2002; Bolte et al., 2004). We previously showed that FM 4-64 is prevented from inserting in IH membranes, which are sealed inside the EIHM (Kankanala et al., 2007). Exclusion of these dyes from fungal membranes was documented by the lack of fluorescent labeling of the fungal septa and vacuoles, which occurs if the dye inserts in the fungal plasma membrane (Atkinson et al., 2002; Kankanala et al., 2007). Infected rice cells treated with FM 4-64 and FM 1-43 showed massive accumulation of these dyes in both tip- and side-BICs (Figure 3D). Images of BICs stained with FM 4-64 showed vesicles carrying effectors immersed in the region of intense staining associated with the BICs (Figure 3E). Vesicles that carry effectors were also observed separated from the BIC, presumably in the rice cytoplasm (Figure 3E, inset upper right), but effector-containing vesicles have not been frequently observed at long distances from the BIC (Supplemental Movie S2). Apparent vesicular bursting was also observed, which suggests that the vesicles are unstable, presumably releasing the effector contents into the host cytoplasm. Taken together, these results indicate that BIC-associated effector vesicles are more likely derived through plant endocytosis than from secretion of fungal exosomes.

Bas83 is a unique cytoplasmic effector that associates with rice membrane concentrating around BICs

Since it is likely that specific blast effectors play roles in vesicle formation and effector translocation, we were particularly interested in effectors that appear to associate with membranes in host cells. The *BAS83* (MGG_08506.6) gene is unique to *M. oryzae*, and it is 36-fold upregulated

during biotrophic invasion (Mosquera et al., 2009). Bas83:mRFP is translocated into invaded host cells, but it does not precisely colocalize with other BIC-localized cytoplasmic effectors Pwl2:eGFP and Pwl1:eGFP (Figure 4A; Supplemental Figure S3). In contrast, Bas83:mRFP seems to label the EIHM surrounding the BIC-associated cells, the primary hyphae and first bulbous IH, and it labels membrane bubbles, or vesicles, near to BICs and BIC-associated cells (Figure 4A-C). Figure 4A shows that Bas83:mRFP-labeled vesicles do not contain the cytoplasmic effector Pwl2:eGFP, indicating they are distinct from effector vesicles in BICs. Bas83:mRFP is also associated with vesicles observed under appressoria (Figure 4C; Supplemental Figure S3). However, Bas83:mRFP fails to label membrane surrounding subsequently formed bulbous IH that are associated with apoplastic effectors and not with cytoplasmic effectors (see 2nd bulbous IH in Figure 4C). We hypothesize that Bas83 is involved in recruiting new plant plasma membrane to form the EIHM and BICs during biotrophic development. However, repeated attempts in two different laboratories (264 purified transformants, 4 methods and 5 experiments; KSU and Univ. of Exeter) failed to produce knock-out mutants for further functional analysis (Supplemental Figure S4).

BICs contain plant actin

The actin cytoskeleton is essential for endocytic processes including plasma membrane folding, vesiculation, and vesicle transport (Grassart et al., 2014; Narasimhan et al., 2020). Effector vesicle formation in BICs suggests that this interfacial structure should contain abundant host actin. Therefore, we imaged plant actin dynamics during biotrophic invasion using rice lines expressing the actin marker LifeAct:eGFP. Infection by *M. oryzae* strains expressing chimeric protein Pwl2:mRFP showed massive colocalization of LifeAct:eGFP in BICs (Figure 5A). Actin was abundant in all imaged tip- and side-BICs (Figure 5B). Likewise, colocalization of fluorescent Phalloidin conjugates and fluorescently-labeled effector confirmed that BICs are rich in plant actin filaments (Figure 5C). We hypothesize that actin filaments are responsible for plasma membrane manipulation, vesiculation and possibly for the transport of vesicles carrying effectors into the rice cell cytoplasm.

BICs consistently contain abundant plant clathrin, but not flotillin

Clathrin-mediated endocytosis (CME) is the major endocytosis mechanism in plants, with some contribution by Clathrin-independent endocytosis (CIE) (Chen et al., 2011; Ewers and Helenius,

2011; Fan et al., 2015; Narasimhan et al., 2020). To assess co-localization of specific endocytosis markers with BICs, we generated transgenic rice lines expressing a fluorescent marker for either CME or CIE. For CME, we generated a C-terminal translational fusion of eGFP with the rice Clathrin light chain-1 (OsCLC1), which is a component of the clathrin coat together with clathrin heavy chain. Rice lines expressing OsCLC1:eGFP show typical clathrin foci (Konopka et al., 2008; Narasimhan et al., 2020) in uninfected rice cells (Figure 6A). The marker for CIE was a C-terminal translational fusion of eGFP to flotillin (Flot1), which is a component of lipid rafts (Otto and Nichols, 2011; Li et al., 2012). Rice lines with the CME and CIE markers were used for leaf sheath assays with an *M. oryzae* strain expressing Pwl2:mRFP to label BICs. In addition to typical clathrin foci around the cell periphery, all tip-BICs and side-BICs contain fluorescence from OsCLC1:eGFP co-localizing with Pwl2:mRFP (Figure 6A,B). Clathrin fluorescence could sometimes be observed co-localizing with effector fluorescence in BIC vesicles (Supplemental Movie S3). In contrast, no tip-BICs colocalized with Flot1:eGFP. Some colocalization of Flot1:eGFP and Pwl2:mRFP occurred in side-BICs besides mature bulbous hyphae (Figure 6B). Colocalization results from several independent experiments were consistent with a major role for CME, but not for CIE, in the internalization of cytoplasmic effectors.

Silencing of rice endocytosis machinery blocks *M. oryzae* infection

We assessed the impact of inhibition of CME and CIE on BICs and effector vesicles using the brome mosaic virus system (Ding et al., 2006; Ding et al., 2007) for silencing of genes for CME and CIE components that have been characterized by gene silencing analyses in *Arabidopsis*. Specifically, we silenced two rice CME genes, Adaptor protein complex-2 subunit α2 (*AP-2α*) and clathrin heavy chain-1 (*CHC1*) (Di Rubbo et al., 2013; Larsson et al., 2017) as well as the CIE gene *Flotillin-1* (*Flot1*) (Li et al., 2012). Silencing of both CME components *AP-2α* and *CHC1* resulted in severe reduction in pathogenicity in whole plant spray inoculation assays (Figure 7A,B). However, as expected, silencing of these genes caused stunting and decreased plant health (Supplemental Figure S5), and levels of pathogenicity in blast disease are known to be decreased on unhealthy rice plants. More significant is the phenotype of pathogen blockage at individual infection sites. Silencing of either CME component RNAi*AP-2α* or RNAi*CHC1* led to a distinctive swollen BIC phenotype, with enlarged, abnormally-shaped BICs that lack effector vesicles (Figure 7C-F). By contrast, silencing of the CIE marker gene *Flot1* showed less severe stunting (Supplemental Figure S5), less of an impact on pathogenicity (Figure 7A,B), and minor impact on

BIC structure (Figure 7C-F). For example, compare the 28 hpi images of BICs in control rice plants with the RNAi*Flot1*-silenced and the RNAi*AP-2*α-silenced rice plants in Figure 7C, and quantification of swollen BIC events in Figure 7F.

In addition to swollen BICs at sites with primary hyphae, silencing of both CME genes decreased appressorial penetration and induced the accumulation of the cytoplasmic effector Pwl2:mRFP under failed penetration sites where it is not normally observed (Figure 7D,E). In contrast, silencing of *Flot1* had only minor effects on appressorium penetration success and on accumulation of Pwl2:mRFP under failed appressoria. Like our finding of early accumulation of Bas170 under appressoria before penetration, these results again suggest that effector uptake begins before host penetration. These results also suggest that CME plays a role in effector translocation at the appressorial penetration stage as well as from BICs.

Chemical inhibition of rice endocytosis machinery blocks *M. oryzae* infection

Pharmacological approaches have impacted studies in diverse biological systems (Robinson et al., 2008; Hicks and Raikhel, 2010; Grassart et al., 2014; Fan et al., 2015). To further assess potential impact of the plant endocytic machinery on cytoplasmic effector translocation, we tested a series of chemicals that are reported to inhibit plant CME or CIE (Table 1). Compared with the non-treated control (Figure 8A), treatment with reported CME inhibitor cantharidin led to abnormally-shaped swollen BICs that lack distinct effector vesicles, resembling those seen with silencing of CME components (Figure 8B). Fluorescence intensity linescans confirm that cantharidin treatment had little, if any, impact on localization of apoplastic effector Bas4:eGFP in the base of the BIC.

Subsequent quantification of cantharidin treatment along with treatment of 2 additional reported CME inhibitors, chlorpromazine and triclosan (Table 1), showed a high proportion of swollen, irregular-shaped cytoplasmic effector fluorescence patterns in BICs (Figure 9A-C). By contrast, inhibition of CIE with filipin and methyl-β-cyclodextrin resulted in minor to no effect on BIC effector fluorescence patterns (Figure 9A-C). Two chemical inhibitors with potential CME association (Table 1) show different impacts on BIC effector fluorescence patterns. Wortmannin, which inhibits phosphatidylinositol 3-kinase (PI 3-kinase) and is implicated in late endosomal trafficking (Robinson et al., 2008) had a major impact on BIC structure, while concanamycin A, which inhibits vacuolar-type ATPase and induces vacuolar acidification (Robinson et al., 2008), had little impact on BIC structure (Figure 9A-C).

Moreover, treatment with CME inhibitors cantharidin, chlorpromazine and triclosan, but not with CIE inhibitors filipin and methyl-β-cyclodextrin, resulted in reduced appressorial penetration and induced abnormal accumulation of the cytoplasmic effector Pwl2:mRFP under appressorial penetration sites where it is not normally observed (Figure 9A - compare 18 hpi CIE and CME inhibitors; Figure 9D,E). Wortmannin, but not concanamycin A, also impacted appressorial function and resulted in abnormal Pwl2:mRFP accumulation under appressoria. These results support our findings with Bas170:mRFP (Figure 1D-F) in suggesting that effector uptake begins before or at the point that host penetration occurs. Indeed, chemical inhibition of endocytosis in rice cells undergoing *M. oryzae* infection mimics the results obtained with VIGS, further supporting a role for CME in effector uptake into rice cells.

DISCUSSION

Our results, when taken together, provide strong evidence that cytoplasmic effector translocation is BIC-localized and mediated by CME. We report that diverse cytoplasmic effectors occur in dynamic vesicles in tip-BICs associated with primary hyphae that first colonize host cells and then in BICs that remain beside the first bulbous IH after hyphal differentiation. Tip-BICs contain many small effector micro-vesicles (~87 nm) and co-expression of differentially-labeled effectors Bas1:eYFP and Pwl2:mRFP showed these effectors can be sorted into different vesicles (Figure 2). Vesicle composition can be seen to vary as tip-BICs move to become side-BICs during hyphal differentiation. Specifically, side-BICs contained fewer, larger vesicles that reach >500 nm in diameter and show co-localization of Bas1:eYFP and Pwl2:mRFP. Our results confirm a previous report that cytoplasmic effectors occur in ~500 nm vesicles in the outer BIC domes beside bulbous IH (Mochizuki et al., 2015; Nishimura et al., 2016; Nishizawa et al., 2016). We also observed effector vesicles in the host cytoplasm at short distances from maturing side-BICs (Figure 2). Release of effectors from these vesicles into the host cytoplasm would require a special mechanism, perhaps mediation by an effector as suggested for release of the *S. parasitica* effector from endocytic vesicles into the fish cell cytoplasm (Trusch et al., 2018).

We report that BICs producing effector vesicles contain multiple hallmarks of active clathrin-mediated endocytosis (CEM), including focal accumulation of fluorescently-labelled Clathrin Light Chain-1 (CLC1), a key subunit of the clathrin coat in CME (Figure 6). Focal accumulation of actin in the BICs, as detected in stable transgenic plants expressing LifeAct:eGFP

and by staining with rhodamine-labeled phalloidin (Figure 5), is consistent with a role in CME, although it was recently reported that actin plays a different role in CME in plants than in the well-studied systems in mammals and yeast (Qi et al., 2018; Johnson et al., 2020; Narasimhan et al., 2020). We confirm that BICs contain abundant rice plasma membrane (Giraldo et al., 2013) using transgenic plants expressing fluorescent plasma membrane fusion protein LTi6b:eGFP, and using the amphiphilic stryryl dyes FM 4-64 or FM 1-43 to track membranes that are internalized by endocytosis (Bolte et al., 2004). Indeed, we obtained occasional views of effector vesicles ringed in LTi6b:eGFP or FM 4-64 labeled membrane (Figure 3C). Interestingly, we identified a novel effector, Bas83, that labels non-effector vesicles and EIHM focused around BICs and the BIC-associated cells, which could be involved in replenishing host membranes needed for extensive endocytotic activity in the BIC (Figure 4; Supplemental Figure S3). In contrast, flotillin (Flot1:eGFP), which is a component of lipid raft-mediated clathrin independent endocytosis, rarely co-localizes with tip-BICs where active translocation is occurring (Figure 6C). Our fluorescent marker co-localization experiments are all consistent with BICs as a focused area of CME.

For functional analyses of the role of endocytosis in effector translocation, we performed transient silencing of two rice CME components, Clathrin Heavy Chain-1 (CHC-1) and Adaptor Protein Complex subunit 2α (AP-2α), as well as silencing of the CIE component Flotillin-1. We also used 7 pharmacological agents that are reported to inhibit or be associated with CME or CIE in plants. Both strategies have potential problems. Rice plants that received the CHC-1 and APC-2 silencing vectors were significantly reduced in rice blast symptom, compared to the empty vector control and to Flot1-silenced lines (Figure 7; Supplemental Figure S5). However, this could be due, at least in part to inevitable health costs to the plant through silencing component genes for essential cellular processes. Unhealthy rice plants are generally less susceptible to blast disease (Kato, 1974). Additionally, care must be taken in the interpretation of results in pharmacological studies based on new evidence that endocytosis inhibitors characterized in mammalian systems may not have the same targets in plants (Dejonghe et al., 2016), and pharmacological agents also have off-target effects (Hicks and Raikhel, 2010; Dejonghe and Russinova, 2017). However, both studies complement each other in that transient silencing of the two CME components and treatment with 4 different pharmacological agents associated with CME gave the same swollen BIC phenotype, in which labeled fluorescent effectors accumulate in abnormally-sized BICs lacking the discreet effector vesicles seen in control infection sites (Figures 7-9). In contrast,

transient silencing of the CIE component Flotilin-1 and treatment with pharmacological inhibitors associated with CIE show little or no impact on BIC vesicular structure and pathogenicity (Figure 8 and 9). All results from our VIGS and chemical inhibitor experiments are consistent with our fluorescence localization experiments. Taken together, our results therefore provide evidence that BICs include a focused region of plant clathrin-mediated endocytosis for internalizing cytoplasmic effectors inside living plant cells (Figure 10).

We report two new lines of evidence that effectors are being secreted and translocated into the host cytoplasm from appressoria even before obvious growth of primary hyphae inside host cells. First, we identified an effector, Bas170, that naturally accumulates in host nuclei before visible growth of primary hyphae, and it also localizes to vesicles underneath appressoria at this early time point. Second, effector Pwl2:mRFP, which is not normally observed before the tip-BIC stage, accumulates under appressoria that failed to penetrate after both VIGS silencing and chemical inhibition of rice CME. These new findings are consistent with reports that rice cells recognize and respond to *M. oryzae* before and independently of appressorial penetration (Xu et al., 1998). It has been predicted that *M. oryzae* appressorial pores, a transient cell wall-less region of the appressorium adjacent to the plant cuticle, might be involved in molecular communication between pathogen and host before penetration (Howard and Valent, 1996). Previously, the only *M. oryzae* effector that was a candidate for secretion through the appressorial pore was a presumed secondary metabolite that is produced by the *AVR* gene *ACE1* encoding a hybrid polyketide synthase (PKS) and nonribosomal peptide synthetase (NRPS) that is specifically expressed in the cytoplasm of appressoria before and during penetration (Fudal et al., 2007; Collemare et al., 2008). Therefore, our new effector localization results suggest similar exquisite staging of effector expression as reported for the crucifer pathogen *Colletotrichum higginsianum*, which secretes ChEC effectors under the appressorial pores and at subsequent stages during the invasion of *Arabidopsis thaliana* cells (Kleemann et al., 2012). Specifically, this fungus focally secreted effectors Chec6 and Chec36 from the appressorium pore, suggesting these effectors may be translocated before fungal penetration (Kleemann et al., 2012). Our results with Bas170 together with ChECs and Ace1 protein localization patterns indicate that many effectors might be focally secreted through appressorial pores (Fudal et al., 2007; Kleemann et al., 2012), highlighting a potential role for fungal appressoria in effector delivery.

The effector vesicle dynamics that we report support the idea that front-loaded effector translocation occurs during the early stages of host cell invasion. Specifically, tip-BIC vesicles are small (~87 nm), abundant and selective in terms of sorting different cytoplasmic effectors, Bas1:eYFP and Pwl2:mRFP, into different vesicles. In contrast, side-BICs contain fewer, larger, less-selective vesicles that contain both Bas1:eYFP and Pwl2:mRFP. Effector vesicles observed in the cytoplasm were almost uniformly found at the side-BIC stage, perhaps indicating a slow-down of the mechanism for effector release from the vesicles as BICs mature. The mechanism for forming vesicles may result in larger vesicles, or vesicles may fuse before releasing effectors to the cytoplasm in the later BIC stages. Slowdown of the translocation system would appear consistent with previous reports of loss of activity in BICs as host cells fill with IH (Khang et al., 2010; Jones et al., 2021). Front-loading effector translocation from BICs would make sense because cell-to-cell movement of blast cytoplasmic effectors through plasmodesmata must occur in the early stages of host cell invasion while the EIHM enclosing the IH remains intact and plasmodesmata in the invaded cell remain open (Sakulkoo et al., 2018; Jones et al., 2021). Active BICs are surrounded by host cytoplasm with dynamic connections to the cell periphery (Khang et al., 2010; Supplemental Movie S2), where cytoplasmic streaming would rapidly disperse effectors to pit fields containing plasmodesmata. In contrast, nonBIC-associated IH cells invaginate the host vacuole and grow in close proximity to the host vacuolar membrane with little surrounding cytoplasm (Mochizuki et al., 2015; Jones et al., 2021). Specifically, the host vacuole remains intact, but shrinks as IH grow. Both the EIHM and vacuolar membrane become disrupted, indicating death of the invaded cell, around the time IH move into neighboring cells to repeat their BIC-mediated invasion strategy (Mochizuki et al., 2015; Jones et al., 2021).

There is evidence supporting occurrence of clathrin-mediated endocytosis at the EHM in one additional pathosystem. That is, transmission electron micrographs of the interfacial matrix between the intracellular hyphae [called monokaryotic (M)-haustoria] of the monokaryotic rust fungus *Uromyces vignae* and its host cowpea (*Vigna unguiculata*) shows clathrin-coated pits (diameter ca. 50-70nm) on the EHM at M-haustoria hyphal tips that contained dense cytoplasm and were presumably growing (Stark-Urnau and Mendgen, 1995). The coated vesicles were labeled by an antibody recognizing the heavy chain subunit of clathrin. Long tubules extending into the host cytoplasm, as well as coated vesicles in the surrounding host cytoplasm, were also labeled with the antibody, indicating that endocytosis occurs at the EHM (Stark-Urnau and

Mendgen, 1995; O'Connell and Panstruga, 2006). It was suggested that these endocytic vesicles might be involved in effector uptake into host cells in addition to membrane recycling from host exocytosis. Unfortunately, lack of transformation capability and identification of effectors makes it difficult to follow up on these intriguing results with *U. vignae*. Additional TEM studies support our results that transient silencing of lipid raft-mediated endocytosis component Flotilin1, as well as filipin treatment, had little effect on BIC structure and effector vesicle formation. Freeze-fracture transmission electron microscopy (TEM) following filipin treatment revealed an absence of granular filipin-sterol complexes on the EHM of two rust fungi, *Puccinia coronata* and *Uromyces appendiculatus* (Harder and Mendgen, 1982), suggesting that the extrahaustorial membrane contains less sterol than normal plasma membranes, and indicating that the EHM appears depleted in sterol-rich lipid rafts.

Differences in infection strategies among various filamentous biotrophic or hemibiotrophic pathogens would be consistent with use of different strategies for effector translocation in different pathosystems. A recent report indicates that a complex of seven proteins from the smut pathogen *U. maydis* is critical for infection and implicated in translocation of cytoplasmic effectors into maize cells (Ludwig et al., 2021). This basidiomycete fungus colonizes host tissue as intracellular hyphae that pass through and between host cells without obviously specialized interfacial zones, and fluorescent fusion proteins of cytoplasmic effectors have not been visualized in the host cell cytoplasm in this pathosystem (Lo Presti et al., 2017). *U. maydis* produces galls on maize seedlings and grows systemically as the plant grows to finally invade ovaries, which swell into dramatic sporulating galls. In contrast, *M. oryzae* densely colonizes a localized tissue area that will become a visible eyespot lesion that releases spores to reinitiate the infection cycle within 7 days. Different pathogenic lifestyles could present different demands for cytoplasmic effector translocation.

Taken together, our data strongly suggest that clathrin-mediated endocytosis occurring in BICs is a key mechanism for internalization of *M. oryzae* effectors inside living rice cells, beginning even before appressorium penetration on the host surface. Given this current understanding, important unknowns for future study include the molecular mechanisms of how the endocytic machinery is recruited to BICs and how it interacts with effector cargos (Qi et al., 2018), including how different effectors are sorted out into different vesicles as shown in Figure 2. It is important to understand vesicle dynamics through time and why effector vesicles become larger and less selective as BICs mature. It is important to understand if, and if so, how, Bas83 contributes

to membrane recruitment to BICs and the EIHM surrounding BIC-associated cells. It is unknown how the effector vesicles are disrupted, releasing effectors into the rice cytoplasm and how various effectors are then targeted to their destinations in host cells including, in some cases, movement through plasmodesmata into neighboring host cells. It is also important to understand the role for appressoria in effector secretion before penetration, and how these early effectors, such as the host nuclear localized effector Bas170, function to promote infection. Finally, it is critical to translate molecular mechanisms of blast biotrophic invasion into strategies for controlling devastating diseases on rice, wheat and other food crops worldwide.

METHODS

Live-cell imaging of *M. oryzae* effectors *in planta*

Fungal strains were stored in dried filter papers at -20˚C, and cultured on rice polish agar plates at 25˚C under continuous light for 2 weeks (Valent and Chumley, 1991). Rice sheath inoculations were performed as described (Kankanala et al., 2007) with the following modification. We used sheath pieces that were thickly trimmed (~7 rice cell layers thick) compared to thinner trimmed sheaths (~3 cell layers thick) in previous publications. Brightfield images are less detailed, but the endocytic machinery appeared more active, providing enhanced microscopic resolution of fluorescent marker dynamics. Susceptible rice variety YT-16 was used unless mentioned otherwise. Briefly, 7-cm-long sheath pieces from 3-week-old plants were placed in a sealable Pyrex glass moist chamber. Leaf sheath sections were placed on inverted 8-well PCR tube strips to avoid contact with wet paper and to hold epidermal cells directly above the mid-vein horizontally flat for uniform inoculum distribution in the trimmed sheath pieces. A spore suspension (10^4 spores/ml in sterile 0.25% gelatin, Cat. #G-6650, Sigma-Aldrich) was prepared from 10-day old cultures and was injected into one end of the sheath using a 100-ml pipette. Each segment was trimmed at 18–30 h.p.i., treated with specific dyes or inhibitors, or imaged immediately by laser confocal microscopy. Confocal imaging was performed with a Zeiss LSM780 confocal microscope system using two water immersion objectives, C-Apochromat 40x/1.2 WCorr. and C-Apochromat 63x/1.2WCorr. Excitation/emission wavelengths were 488 nm/505–550 nm for eGFP and FM1-43, and 543 nm/560–615 nm for mRFP, mCherry, Phalloidin and FM4-64. Images were acquired and processed using Zeiss ZEN 2010 software. Images of effector vesicles in Figure 3C were obtained using a Leica SP8 confocal microscope system with

a water immersion objective HC PL APO 63x/1.20 WCorr. Excitation/emission wavelengths were 488 nm/505–550 nm for eGFP and 543 nm/560–615 nm for mRFP.

Fungal strains, DNA manipulation, and fungal transformation

Magnaporthe oryzae wild type strain Guy11, a field isolate from rice in French Guiana, was obtained from J.L. Notteghem (Centre de Cooperation Internationale en Recherche Agronomique pour le Developpment). *M. oryzae* transformants are described in Supplemental Table S1 online. Effector:mRFP and Effector:eGFP expression plasmids were constructed by PCR amplifying different effector gene regions and fusing them to the N-terminus of mRFP and eGFP, respectively. Details of construction of each plasmid are described in Supplemental Table S2, and primers are listed in Supplemental Table S3. For all fusion constructs, transcriptional and translational fusions were verified by DNA sequencing. See Supplemental Table S2 online for plasmids used, and Supplemental Table S3 for PCR primers used. Plasmids were transformed into laboratory strain Guy11 (Leung et al., 1988) using *Agrobacterium tumefaciens*–mediated transformation (Khang et al., 2006). In several cases, two fluorescently labelled effectors were introduced by co-transformation with separate plasmids (Sweigard et al., 1995). Because positive transformants showed similar fluorescence patterns with varying intensities, those with strongest fluorescence were studied (see Supplemental Table S1 online). For each construct cloned in *M. oryzae*, at least two independent transformants showing identical phenotypes to the wild type were selected and assayed together.

Strategies for targeted deletion of Bas83 gene

Split-marker recombination method for Bas83 gene knockout via protoplast transformation: Targeted gene replacement mutation of the *M. oryzae Bas83* gene was attempted using the split marker strategy as modified by Kershaw and Talbot (2009). Gene replacement was performed by replacing the 606-bp *Bas83* locus with a hygromycin resistance selectable marker, encoding a 1.4-kb hygromycin phosphotransferase (*HPH*) resistance cassette (Carroll et al., 1994). The two overlapping segments of the *HPH* templates were PCR amplified using primers M13F with HY and M13R with YG (Catlett et al., 2003) (see Supplemental Table S3 online) as described previously (Kershaw and Talbot, 2009). One-kb DNA fragments upstream and downstream of the *Bas83* open reading frame were generated using the primers Bas83LF-F and Bas83LFHY-R and Bas83RFYG-F and Bas83RF-R amplified from genomic DNA of the Guy11 strain. A second-

round PCR reaction was performed to fuse the overlapping split hph marker templates with the left and right flanking regions of the Bas83 locus. Wild-type *M. oryzae* strain Guy11 was then transformed with the deletion cassettes (2 µg of each flank). Putative transformants were selected in the presence of hygromycin B (200 µg/ml) and analyzed by PCR using the primers Bas83:BASKOtest-F and Bas83:BASKOtest-R (Supplemental Table S3; Supplemental Figure S4). This assay was repeated three times. Gene sequences on either side of *Bas83* were retrieved from the NCBI database (https://www.ncbi.nlm.nih.gov/).

Attempted Bas83 deletion via Agrobacterium-mediated transformation: For gene replacement transformation, cassettes were constructed by amplifying ~1.0 kb of 5′- and 3′-flanking regions for each predicted coding sequence. The *HPH* gene (Carroll et al., 1994) was cloned between the two flanking regions using a fusion PCR strategy. The three pieces together were cloned first into the pJET1.6 vector (Invitrogen) for sequence analysis and later into binary vector pGKO2 (Addgene: Plasmid #63617; Khang et al., 2005) using a restriction ligation strategy. *M. oryzae* KU70 and KU80 spores were transformed using *A. tumefaciens* (Khang et al., 2005) strains AGL1 and EHA105 (Hellens et al., 2000). After two rounds of selection in TB3 media containing 200 µg/mL of hygromycin, 400 independent fungal transformants were analyzed for gene replacement events by PCR amplification using the primers Bas83:BASKOtest-F and Bas83:BASKOtest-R (Supplemental Figure S4). This assay was repeated three times.

Staining with FM 4-64, FM 1-43, and Rhodamine Phalloidin, and treatment with pharmacological inhibitors

To examine membrane dynamics at the BIC, rice sheaths (cv. YT16) were inoculated with *M. oryzae* transformants expressing fluorescently-labeled effectors ($2x10^4$ spores/ml in 0.25% gelatin solution) and incubated for 20-26 hours at 25˚C for subsequent FM-dye treatment. Infected rice sheaths were treated with FM 4-64 or FM 1-43 (4 mg/ml in water). An aqueous 17mM stock solution of FM 4-64 (Cat #13320, Invitrogen, Carlsbad, CA) and FM 1-43 (Cat # T3163, Invitrogen, Carlsbad, CA) were prepared and stored at -20˚C as described (45). *In planta*, inoculated leaf sheaths, 24 h.p.i., were trimmed into ultrathin sections (2-3 layers of cells; 10 x 10 mm) and incubated in a 10-mM aqueous working solution for 3–5 hours. Leaf sheaf sections were subsequently transferred to ultrapure water and incubated for 20 min (25 ˚C) to remove excess dyes for uniform membrane staining. For *in planta* experiments with Rhodamine Phalloidin (Cat# R415, ThermoFisher Scientific), we prepared working solutions of 66 µM in 0.1% DMSO and

treated the inoculated tissue as described for FM dyes.

To examine the effects of endocytosis inhibitors on *in planta* effector uptake, inoculated trimmed rice sheaths were incubated at 25˚C with Methyl-β-cyclodextrin (20 mM), or Chlorpromazine (10 µg/mL), or Cantharidin (25 mM), or Fluazinam (20 mM), or Triclosan (20mM), or Wortmannin (20 nM), or Concanamycin A (50 mM) (all from Sigma) solution for 1-5 hours. Negative controls were performed with ultrapure water (Methyl-β-cyclodextrin, Chlorpromazine, and Fluazinam) or 0.1% DMSO (Cantharidin, Filipin and Wortamanin) (see Table 1).

Generation of transgenic rice plants

Production of transgenic plants expressing the plant plasma membrane marker low-temperature inducible protein 6B, LTi6B:GFP was previously described (Mentlak et al., 2012; Giraldo et al., 2013). Transformants of rice cultivar Sasanishiki expressing LifeAct:eGFP were generated in the laboratory of NJT. Expression plasmids for CME and CIE marker genes were constructed by PCR amplifying the marker gene regions and fusing them to the N-terminus of eGFP. The *CLC1* gene was amplified from genomic DNA of YT16 rice using the primers KpnI_OsCLC1Prom1-F1 and XhoI_OsCLC1-R1. The PCR product was digested with *Kpn*I and *Xho*I and integrated into pSH1.6EGFP (Plasmid #42323, Addgene). The *Flot1* gene was amplified from genomic DNA from YT16 rice using the primers HindIII_OsFlot1Prom1-F1 and Eco47III_OsFlot-R1. The PCR product was digested with *Hind*III and *Eco*47III and integrated into pSH1.6EGFP. CLC1:eGFP was amplified from pSH1.6_CLC1:eGFP using the primers CACC_OsCLC1-F1 and eGFPT2-R2, and cloned into pENTR (pENTR™/D-TOPO™ Cloning Kit, ThermoFisher Scientific) following the manufacturer's protocol. Flot1:eGFP was amplified form pSH1.6_Flot1:eGFP using the primers CACC_OsFlot1-F1 and eGFPT2-R2, and cloned into pENTR following manufacturer's protocols. Endocytosis marker:eGFP construct were cloned into the *Agrobacterium* vector pIPKb001 (Himmelbach et al., 2007) using the Gateway LR Clonase II kit (Invitrogen) following the manufacturer's protocol. All the fusion constructs had transcriptional and translational fusions verified by DNA sequencing. Gene fusions for expressing the rice endocytosis markers CLC1:eGFP (CME) and Flot1:eGFP (CIE) under their native promoters were introduced into *Agrobacterium tumefaciens* EHA105 using the freeze-thaw method (Holsters et al., 1978). Mature seed-derived callus from rice (*Oryza sativa L. Japonica*) cv. YT16 was used for *Agrobacterium*-mediated transformation (Park et al., 2001). After inoculating with *A. tumefaciens*, callus was

transferred to regeneration medium for 4-10 weeks at 25˚C under a 16-h photoperiod. The regenerated shoots were transferred to rooting medium for four more weeks, then established in soil. Putative transformants of rice were selected on 100 µg/ml hygromycin, and expression checked by qRT–PCR and epifluorescence microscopy.

Silencing of rice genes

In order to evaluate the role of plant endocytosis on disease development and effector uptake, we performed VIGS using the Brome mosaic virus system developed by R.S. Nelson (Noble Foundation, Ardmore, OK). We targeted *AP-2α*, *CHC1* (CME) and *Flot1* (CIE) mRNA in rice plants (cultivar IR64) undergoing infection. The target rice sequences were cloned in the pC13/F3-13m VIGS vector as described (Ding et al., 2006; Ding et al., 2007) and subsequently sequenced to verify sequence accuracy. RNA transcripts were synthesized from the final VIGS vector. An empty vector pC13/F3-13m was used as negative control. The final infectious transcripts of pC13/F3-13m / AP-2α, pC13/F3-13m / CHC1, pC13/F3-13m /Flot1 and pC13/F3-13m (a control virus without an insert) were inoculated with pC13/F1+2 in 7 to 10 day old IR64 rice plants according protocols described by Ding et al (2006). Knockdown of the target genes was confirmed by qRT-PCR at 15 days post inoculation. At this point, rice plants showing satisfactory reduction of the transcription levels were used in our standard conidial spray inoculation and leaf sheath assays with fungal strains expressing fluorescently-labeled effectors.

Statistics

All experiments were performed in triplicate and repeated three times. The sample sizes, number of biological and technical replicates, and the statistical tests used in each experiment are specified in the figure legends. Data were analyzed using an unpaired two-tailed Student's t-test. P=0.05 was considered non-significant and exact values are shown where appropriate. All statistical analysis was performed using R Statistical Software (version 4.1.2) and Prism9 (GraphPad). The linescans in Figure 8 were used to illustrate cytoplasmic effector accumulation due to CME inhibition and compared to the apoplastic effector Bas4 (control). Dot plots were routinely used to show individual data points and generated using Prism9 (GraphPad). Bar graphs show the mean±s.e.m. (unless stated otherwise) and were generated using Prism9 (GraphPad). Analysis of non-normal datasets are represented by box-and-whisker plots that show the 25th and 75th

percentiles, the median indicated by a horizontal line, and the minimum and maximum values indicated by the ends of the whiskers.

Accession Numbers

Sequence data for genes of *M. oryzae* used in this article can be found in the GenBank/EMBL database under the following accession numbers: BAS1, NC_017844; PWL1, U36923.1; PWL2, NC_017853; Bas4, NC_017852.1; BAS83, NC_017851.1; BAS170, NC_017850.1. Rice genes used are: Clathrin Light Chain-1 (CLC1), LOC4337419; Flotilin 1 (Flot1), LOC4348926; Adaptor protein complex-2α (AP-2α), LOC4331370; and Clathrin Heavy Chain-1 (CHC1 gene; LOC4349546.

ACKNOWLEDGEMENTS

We acknowledge and thank Rick Nelson (Noble Foundation, Ardmore, OK) for providing the VIGS vectors and hosting E.O.-G. in his laboratory to learn the VIGS assay. We thank the Talbot laboratory for assistance and hospitality during a working visit for E.O.-G at the University of Exeter. We thank Hiromasa Saitoh (Iwate Biotechnology Research Center, Kitakami, Iwate, Japan) and Ryohei Terauchi (Iwate Biotechnology Research Center, Kitakami, Iwate, and Kyoto University, Japan) for sharing transgenic rice expressing plant plasma membrane marker LTi6B:GFP. This project was supported by Agriculture and Food Research Initiative Competitive Grant no. #2017-67013-26525 from the USDA National Institute of Food and Agriculture Plant Biotic Interactions program. This is Contribution no. 22-053-J from the Kansas Agricultural Experiment Station.

AUTHOR CONTRIBUTIONS

E.O.-G. and B.V. designed experiments and analyzed data: E.O.-G. performed most of the research. T.M.T., J.P. and S.P. produced and analyzed transgenic rice lines expressing the rice CLC1:eGFP and Flot1:eGFP fluorescent fusion protein genes. M.D., M.M.-U., C.R.H. and A.H.V. assisted with microscopy and Bas83 Knockout experiments and general laboratory experiments; N.J.T. provided transgenic rice lines expressing LTi6B:GFP and LifeACT:GFP; E.O.-G., B.V. and N.J.T wrote and edited the article.

REFERENCES

Atkinson, H.A., Daniels, A., and Read, N.D. 2002. Live-cell imaging of endocytosis during conidial germination in the rice blast fungus, *Magnaporthe grisea*. Fungal Gen. Biol. 37:233-244.

Beck, M., Heard, W., Mbengue, M., and Robatzek, S. 2012. The INs and OUTs of pattern recognition receptors at the cell surface. Curr. Opin. Plant Biol. 15:367-374.

Bolte, S., Talbot, C., Boutte, Y., Catrice, O., Read, N.D., and Satiat-Jeunemaitre, B. 2004. FM-dyes as experimental probes for dissecting vesicle trafficking in living plant cells. Journal of Microscopy 214:159-173.

Bozkurt, T.O., Belhaj, K., Dagdas, Y.F., Chaparro-Garcia, A., Wu, C.-H., Cano, L.M., and Kamoun, S. 2015. Rerouting of plant late endocytic trafficking toward a pathogen interface. Traffic 16:204-226.

Bright, N.A., Lindsay, M.R., Stewart, A., and Luzio, J.P. 2001. The relationship between lumenal and limiting membranes in swollen late endocytic compartments formed after wortmannin treatment or sucrose accumulation. Traffic 2:631-642.

Carroll, A., Sweigard, J. A., and Valent, B. 1994. Improved vectors for selecting resistance to hygromycin. 41:Article 5. https://newprairiepress.org/fgr/vol41/iss41/45/.

Catlett, N. L., Lee, B.-N., Yoder, O. C., and Turgeon, B. G. 2003. Split-marker recombination for efficient targeted deletion of fungal genes. Fungal Genetics Newsletter 50:Article 4. https://doi.org/10.4148/1941-4765.1150.

Chaparro-Garcia, A., Schwizer, S., Sklenar, J., Yoshida, K., Petre, B., Bos, J.I.B., Schornack, S., Jones, A.M.E., Bozkurt, T.O., and Kamoun, S. 2015. *Phytophthora infestans* RXLR-WY effector AVR3a associates with dynamin-related protein 2 required for endocytosis of the plant pattern recognition receptor FLS2. PLoS ONE 10:e0137071.

Chen, X., Irani, N.G., and Friml, J. 2011. Clathrin-mediated endocytosis: the gateway into plant cells. Curr. Opin. Plant Biol. 14:674-682.

Collemare, J., Pianfetti, M., Houlle, A.E., Morin, D., Camborde, L., Gagey, M.J., Barbisan, C., Fudal, I., Lebrun, M.H., and Böhnert, H.U. 2008. *Magnaporthe grisea* avirulence gene *ACE1* belongs to an infection-specific gene cluster involved in secondary metabolism. New Phytol. 179:196-208.

Dagdas, Y.F., Pandey, P., Tumtas, Y., Sanguankiattichai, N., Belhaj, K., Duggan, C., Leary, A.Y., Segretin, M.E., Contreras, M.P., Savage, Z., Khandare, V.S., Kamoun, S., and Bozkurt, T.O. 2018. Host autophagy machinery is diverted to the pathogen interface to mediate focal defense responses against the Irish potato famine pathogen. eLife 7:e37476.

Dejonghe, W., and Russinova, E. 2017. Plant chemical genetics: From phenotype-based screens to synthetic biology. Plant Physiology 174:5-20.

Dejonghe, W., Kuenen, S., Mylle, E., Vasileva, M., Keech, O., Viotti, C., Swerts, J., Fendrych, M., Ortiz-Morea, F.A., Mishev, K., Delang, S., Scholl, S., Zarza, X., Heilmann, M., Kourelis, J., Kasprowicz, J., Nguyen, L.S.L., Drozdzecki, A., Van Houtte, I., Szatmári, A.-M., Majda, M., Baisa, G., Bednarek, S.Y., Robert, S., Audenaert, D., Testerink, C., Munnik, T., Van Damme, D., Heilmann, I., Schumacher, K., Winne, J., Friml, J., Verstreken, P., and Russinova, E. 2016. Mitochondrial uncouplers inhibit clathrin-mediated endocytosis largely through cytoplasmic acidification. Nat. Comm. 7:11710.

Di Rubbo, S., Irani, N. G., Kim, S. Y., Xu, Z.-Y., Gadeyne, A., Dejonghe, W., Vanhoutte, I., Persiau, G., Eeckhout, D., Simon, S., Song, K., Kleine-Vehn, J., Friml, J., De Jaeger, G., Van Damme, D., Hwang, I., and Russinova, E. 2013. The Clathrin Adaptor Complex AP-2 mediates endocytosis of BRASSINOSTEROID INSENSITIVE1 in *Arabidopsis*. Plant Cell 25:2986-2997.

Ding, X.S., Rao, C.S., and Nelson, R.S. 2007. Analysis of gene function in rice through virus-induced gene silencing. Methods in molecular biology (Clifton, N.J.) 354:145-160.

Ding, X.S., Schneider, W.L., Chaluvadi, S.R., Mian, M.A.R., and Nelson, R.S. 2006. Characterization of a Brome mosaic virus strain and its use as a vector for gene silencing in monocotyledonous hosts. Mol. Plant-Microbe Interact. 19:1229-1239.

Dodds, P.N., and Rathjen, J.P. 2010. Plant immunity: towards an integrated view of plant-pathogen interactions. Nat. Rev. Genet. 11:539-548.

Elsworth, B., Matthews, K., Nie, C.Q., Kalanon, M., Charnaud, S.C., Sanders, P.R., Chisholm, S.A., Counihan, N.A., Shaw, P.J., Pino, P., Chan, J.A., Azevedo, M.F., Rogerson, S.J., Beeson, J.G., Crabb, B.S., Gilson, P.R., and de Koning-Ward, T.F. 2014. PTEX is an essential nexus for protein export in malaria parasites. Nature 511:587-+.

Ewers, H., and Helenius, A. 2011. Lipid-mediated endocytosis. Cold Spring Harbor Perspectives in Biology 3:10.1101/cshperspect.a004721.

Fan, L., Li, R., Pan, J., Ding, Z., and Lin, J. 2015. Endocytosis and its regulation in plants. Trends in Plant Science 20:388-397.

Fawke, S., Doumane, M., and Schornack, S. 2015. Oomycete interactions with plants: infection strategies and resistance principles. Microbiology and Molecular Biology Reviews 79:263-280.

Fudal, I., Collemare, J., Böhnert, H.U., Melayah, D., and Lebrun, M.-H. 2007. Expression of *Magnaporthe grisea* avirulence gene *ACE1* is connected to the initiation of appressorium-mediated penetration. Eukaryotic Cell 6:546-554.

Giraldo, M.C., and Valent, B. 2013. Filamentous plant pathogen effectors in action. Nat. Rev. Microbiol. 11:800-814.

Giraldo, M.C., Dagdas, Y.F., Gupta, Y.K., Mentlak, T.A., Yi, M., Martinez-Rocha, A.L., Saitoh, H., Terauchi, R., Talbot, N.J., and Valent, B. 2013. Two distinct secretion systems facilitate tissue invasion by the rice blast fungus *Magnaporthe oryzae*. Nat. Comm. 4:1996.

Gladieux, P., Condon, B., Ravel, S., Soanes, D., Maciel, J.L.N., Nhani, A., Chen, L., Terauchi, R., Lebrun, M.-H., Tharreau, D., Mitchell, T., Pedley, K.F., Valent, B., Talbot, N.J., Farman, M., and Fournier, E. 2018. Gene flow between divergent cereal- and grass-specific lineages of the rice blast fungus *Magnaporthe oryzae*. mBio 9:e01219-01217.

Grassart, A., Cheng, A.T., Hong, S.H., Zhang, F., Zenzer, N., Feng, Y., Briner, D.M., Davis, G.D., Malkov, D., and Drubin, D.G. 2014. Actin and dynamin2 dynamics and interplay during clathrin-mediated endocytosis. Journal of Cell Biology 205:721-735.

Harder, D.E., and Mendgen, K. 1982. Filipin-sterol complexes in bean rust- and oat crown rust-fungal/plant interactions: Freeze-etch electron microscopy. Protoplasma 112:46-54.

Hellens, R., Mullineaux, P., and Klee, H. 2000. Technical Focus: a guide to *Agrobacterium* binary Ti vectors. Trends Plant Sci. 5:446-451.

Hicks, G.R., and Raikhel, N.V. 2010. Advances in dissecting endomembrane trafficking with small molecules. Curr. Opin. Plant Biol. 13:706-713.

Himmelbach, A., Zierold, U., Hensel, G., Riechen, J., Douchkov, D., Schweizer, P., and Kumlehn, J. 2007. A set of modular binary vectors for transformation of cereals. Plant Physiology 145:1192-1200.

Holsters, M., de Waele, D., Depicker, A., Messens, E., van Montagu, M., and Schell, J. 1978. Transfection and transformation of *Agrobacterium tumefaciens*. Molecular and General Genetics 163:181-187.

Howard, R.J., and Valent, B. 1996. Breaking and Entering: Host penetration by the fungal rice blast pathogen *Magnaporthe grisea*. Annu. Rev. Microbiol. 50:491-512.

Johnson, A., Gnyliukh, N., Kaufmann, W.A., Narasimhan, M., Vert, G., Bednarek, S.Y., and Friml, J. 2020. Experimental toolbox for quantitative evaluation of clathrin-mediated endocytosis in the plant model *Arabidopsis*. Journal of Cell Science 133:jcs248062.

Jones, K., Zhu, J., Jenkinson, C.B., Kim, D.W., Pfeifer, M.A., and Khang, C.H. 2021. Disruption of the interfacial membrane leads to *Magnaporthe oryzae* effector re-location and lifestyle switch during rice blast disease. Frontiers in Cell and Developmental Biology 9:10.3389/fcell.2021.681734.

Kaksonen, M., and Roux, A. 2018. Mechanisms of clathrin-mediated endocytosis. Nat. Rev. Mol. Cell Biol. 19:313-326.

Kale, S.D., Gu, B., Capelluto, D.G.S., Dou, D., Feldman, E., Rumore, A., Arredondo, F.D., Hanlon, R., Fudal, I., Rouxel, T., Lawrence, C.B., Shan, W., and Tyler, B.M. 2010. External lipid PI3P mediates entry of eukaryotic pathogen effectors into plant and animal host cells. Cell 142:284-295.

Kankanala, P., Czymmek, K., and Valent, B. 2007. Roles for rice membrane dynamics and plasmodesmata during biotrophic invasion by the blast fungus. Plant Cell 19:706-724.

Kato, H. 1974. Epidemiology of rice blast disease. Review of Plant Protection Research 7:1-20.

Kershaw, M. J., and Talbot, N. J. 2009. Genome-wide functional analysis reveals that infection-associated fungal autophagy is necessary for rice blast disease. Proceedings of the National Academy of Sciences U.S.A. 106:15967-15972.

Khang, C.H., Park, S., Rho, H., Lee, Y., and Kang, S. 2006. *Agrobacterium tumefaciens*-mediated transformation and mutagenesis of filamentous fungi *Magnaporthe grisea* and *Fusarium oxysporum*. in: Agrobacterium Protocols, K. Wang, ed. Humana Press, Totowa.

Khang, C.H., Berruyer, R., Giraldo, M.C., Kankanala, P., Park, S.-Y., Czymmek, K., Kang, S., and Valent, B. 2010. Translocation of *Magnaporthe oryzae* effectors into rice cells and their subsequent cell-to-cell movement. Plant Cell 22:1388-1403.

Kleemann, J., Rincon-Rivera, L.J., Takahara, H., Neumann, U., Ver Loren van Themaat, E., van der Does, H.C., Hacquard, S., Stüber, K., Will, I., Schmalenbach, W., Schmelzer, E., and O'Connell, R.J. 2012. Sequential delivery of host-induced virulence effectors by appressoria and intracellular hyphae of the phytopathogen *Colletotrichum higginsianum*. PLoS Path. 8:e1002643.

Konopka, C.A., Backues, S.K., and Bednarek, S.Y. 2008. Dynamics of Arabidopsis Dynamin-Related Protein 1C and a Clathrin Light Chain at the plasma membrane. Plant Cell 20:1363-1380.

Larson, E. R., Van Zelm, E., Roux, C., Marion-Poll, A., and Blatt, M. R. 2017. Clathrin heavy chain subunits coordinate endo- and exocytic traffic and affect stomatal movement. Plant Physiol. 175:708-720.

Leung, H., Borromeo, E.S., Bernardo, M.A., and Notteghem, J.L. 1988. Genetic analysis of virulence in the rice blast fungus *Magnaporthe grisea*. Phytopathology 78:1227-1233.

Li, R., Liu, P., Wan, Y., Chen, T., Wang, Q., Mettbach, U., Baluška, F., Samaj, J., Fang, X., Lucas, W.J., and Lin, J. 2012. A membrane microdomain-associated protein, *Arabidopsis* Flot1, is involved in a clathrin-independent endocytic pathway and is required for seedling development. Plant Cell 24 2105-2122

Lo Presti, L., and Kahmann, R. 2017. How filamentous plant pathogen effectors are translocated to host cells. Curr. Opin. Plant Biol. 38:19-24.

Lo Presti, L., Zechmann, B., Kumlehn, J., Liang, L., Lanver, D., Tanaka, S., Bock, R., and Kahmann, R. 2017. An assay for entry of secreted fungal effectors into plant cells. New Phytol. 213:956-964.

Lo Presti, L., Lanver, D., Schweizer, G., Tanaka, S., Liang, L., Tollot, M., Zuccaro, A., Reissmann, S., and Kahmann, R. 2015. Fungal effectors and plant susceptibility. Annual Review of Plant Biology 66:513-545.

Ludwig, N., Reissmann, S., Schipper, K., Gonzalez, C., Assmann, D., Glatter, T., Moretti, M., Ma, L.-S., Rexer, K.-H., Snetselaar, K., and Kahmann, R. 2021. A cell surface-exposed protein complex with an essential virulence function in *Ustilago maydis*. Nature Microbiology 6:722-730.

Manning, V.A., and Ciuffetti, L.M. 2005. Localization of Ptr ToxA produced by *Pyrenophora tritici-repentis* reveals protein import into wheat mesophyll cells. Plant Cell 17:3203-3212.

Maranda, B., Brown, D., Bourgoin, S., Casanova, J.E., Vinay, P., Ausiello, D.A., and Marshansky, V. 2001. Intra-endosomal pH-sensitive recruitment of the Arf-nucleotide exchange factor ARNO and Arf6 from cytoplasm to proximal tubule endosomes. Journal of Biological Chemistry 276:18540-18550.

Mbengue, M., Bourdais, G., Gervasi, F., Beck, M., Zhou, J., Spallek, T., Bartels, S., Boller, T., Ueda, T., Kuhn, H., and Robatzek, S. 2016. Clathrin-dependent endocytosis is required for immunity mediated by pattern recognition receptor kinases. Proceedings of the National Academy of Sciences 113:11034-11039.

Mentlak, T.A., Kombrink, A., Shinya, T., Ryder, L.S., Otomo, I., Saitoh, H., Terauchi, R., Nishizawa, Y., Shibuya, N., Thomma, B.P., and Talbot, N.J. 2012. Effector-mediated suppression of chitin-triggered immunity by *Magnaporthe oryzae* is necessary for rice blast disease. Plant Cell 24:322-335.

Mochizuki, S., Minami, E., and Nishizawa, Y. 2015. Live-cell imaging of rice cytological changes reveals the importance of host vacuole maintenance for biotrophic invasion by blast fungus, *Magnaporthe oryzae*. MicrobiologyOpen 4:952-966.

Mosquera, G., Giraldo, M.C., Khang, C.H., Coughlan, S., and Valent, B. 2009. Interaction transcriptome analysis identifies *Magnaporthe oryzae* BAS1-4 as biotrophy-associated secreted proteins in rice blast disease. Plant Cell 21:1273-1290.

Narasimhan, M., Johnson, A., Prizak, R., Kaufmann, W.A., Tan, S., Casillas-Pérez, B., and Friml, J. 2020. Evolutionarily unique mechanistic framework of clathrin-mediated endocytosis in plants. eLife 9:e52067.

Nishimura, T., Mochizuki, S., Ishii-Minami, N., Fujisawa, Y., Kawahara, Y., Yoshida, Y., Okada, K., Ando, S., Matsumura, H., Terauchi, R., Minami, E., and Nishizawa, Y. 2016. *Magnaporthe oryzae* glycine-rich secretion protein, Rbf1 critically participates in pathogenicity through the focal formation of the biotrophic interfacial complex. PLoS Path. 12:e1005921.

Nishizawa, Y., Mochizuki, S., Yokotani, N., Nishimura, T., and Minami, E. 2016. Molecular and cellular analysis of the biotrophic interaction between rice and *Magnaporthe oryzae* – Exploring situations in which the blast fungus controls the infection. Physiol. Mol. Plant Pathol. 95:70-76.

O'Connell, R.J., and Panstruga, R. 2006. Tête à tête inside a plant cell: establishing compatibility between plants and biotrophic fungi and oomycetes. New Phytol. 171:699-718.

Otto, G.P., and Nichols, B.J. 2011. The roles of flotillin microdomains – endocytosis and beyond. Journal of Cell Science 124:3933-3940.

Park, S.H., Park, J., and Smith, R.H. 2001. Herbicide and insect resistant elite transgenic rice. Journal of Plant Physiology 158:1221-1226.

Petre, B., and Kamoun, S. 2014. How do filamentous pathogens deliver effector proteins into plant cells? PLoS. Biol. 12:e1001801.

Petre, B., Contreras, M.P., Bozkurt, T.O., Schattat, M.H., Sklenar, J., Schornack, S., Abd-El-Haliem, A., Castells-Graells, R., Lozano-Durán, R., Dagdas, Y.F., Menke, F.L.H., Jones, A.M.E., Vossen, J.H., Robatzek, S., Kamoun, S., and Win, J. 2021. Host-interactor screens of *Phytophthora infestans* RXLR proteins reveal vesicle trafficking as a major effector-targeted process. Plant Cell 33:1447-1471.

Postma, J., Liebrand, T.W.H., Bi, G., Evrard, A., Bye, R.R., Mbengue, M., Kuhn, H., Joosten, M.H.A.J., and Robatzek, S. 2016. Avr4 promotes Cf-4 receptor-like protein association with the BAK1/SERK3 receptor-like kinase to initiate receptor endocytosis and plant immunity. New Phytol. 210:627-642.

Qi, X., Pleskot, R., Irani, N.G., and Van Damme, D. 2018. Meeting report – Cellular gateways: expanding the role of endocytosis in plant development. Journal of Cell Science 131:jcs222604.

Reynolds, G.D., Wang, C., Pan, J., and Bednarek, S.Y. 2018. Inroads into internalization: Five years of endocytic exploration. Plant Physiology 176:208-218.

Robinson, D.G., Jiang, L.W., and Schumacher, K. 2008. The endosomal system of plants: Charting new and familiar territories. Plant Physiology 147:1482-1492.

Rodal, S.K., Skretting, G., Garred, O., Vilhardt, F., van Deurs, B., and Sandvig, K. 1999. Extraction of cholesterol with methyl-beta-cyclodextrin perturbs formation of clathrin-coated endocytic vesicles. Molecular Biology of the Cell 10:961-974.

Sachse, M., Urbe, S., Oorschot, V., Strous, G.J., and Klumperman, J. 2002. Bilayered clathrin coats on endosomal vacuoles are involved in protein sorting toward lysosomes Molecular Biology of the Cell 13:1313-1328

Sakulkoo, W., Oses-Ruiz, M., Garcia, E.O., Soanes, D.M., Littlejohn, G.R., Hacker, C., Correia, A., Valent, B., and Talbot, N.J. 2018. A single fungal MAP kinase controls plant cell-to-cell invasion by the rice blast fungus. Science 359:1399-1403.

Serrano, M., Robatzek, S., Torres, M., Kombrink, E., Somssich, I.E., Robinson, M., and Schulze-Lefert, P. 2007. Chemical interference of pathogen-associated molecular pattern-triggered immune responses in Arabidopsis reveals a potential role for fatty-acid synthase type II complexderived lipid signals. Journal of Biological Chemistry 282:6803-6811.

Spallek, T., Beck, M., Ben Khaled, S., Salomon, S., Bourdais, G., Schellmann, S., and Robatzek, S. 2013. ESCRT-I mediates FLS2 endosomal sorting and plant immunity. PLoS Genetics 9:e1004035.

Stark-Urnau, M., and Mendgen, K. 1995. Sequential deposition of plant glycoproteins and polysaccharides at the host-parasite interface of *Uromyces vignae* and *Vigna sinensis*: Evidence for endocytosis and secretion. Protoplasma 186:1-11.

Sweigard, J. A., Carroll, A. M., Kang, S., Farrall, L., Chumley, F. G., and Valent, B. 1995. Identification, cloning, and characterization of *PWL2*, a gene for host species specificity in the rice blast fungus. Plant Cell 7:1221-1233.

Trusch, F., Loebach, L., Wawra, S., Durward, E., Wuensch, A., Iberahim, N.A., de Bruijn, I., MacKenzie, K., Willems, A., Toloczko, A., Diéguez-Uribeondo, J., Rasmussen, T., Schrader, T., Bayer, P., Secombes, C.J., and van West, P. 2018. Cell entry of a host-targeting protein of oomycetes requires gp96. Nat. Comm. 9:2347.

Valent, B., and Chumley, F.G. 1991. Molecular genetic analysis of the rice blast fungus, *Magnaporthe grisea*. Annu. Rev. Phytopathol. 29:443-467.

Valent, B., Singh, P.K., He, X., Farman, M., Tosa, Y., and Braun, H.J. 2020. Blast diseases: Evolution and challenges of a staple food crop fungal pathogen. Pages 267-292 in: Emerging Plant Diseases and Global Food Security, J.B. Ristaino and A. Records, eds. American Phytopathological Society Press, St. Paul, MN.

Van den Ackerveken, G. 2017. Seeing is believing: imaging the delivery of pathogen effectors during plant infection. New Phytol. 216:8-10.

Wang, L.H., Rothberg, K.G., and Anderson, R.G. 1993. Misassembly of clathrin lattices on endosomes reveals a regulatory switch for coated pit formation Journal of Cell Biology 123:1107-1117.

Wang, S., Boevink, P.C., Welsh, L., Zhang, R., Whisson, S.C., and Birch, P.R.J. 2017. Delivery of cytoplasmic and apoplastic effectors from *Phytophthora infestans* haustoria by distinct secretion pathways. New Phytol. 216:205-215.

Wawra, S., Trusch, F., Matena, A., Apostolakis, K., Linne, U., Zhukov, I., Stanek, J., Koźmiński, W., Davidson, I., Secombes, C.J., Bayer, P., and van West, P. 2017. The RxLR motif of the host targeting effector AVR3a of *Phytophthora infestans* is cleaved before secretion. Plant Cell 29:1184-1195.

Xu, J.-R., Staiger, C.J., and Hamer, J.E. 1998. Inactivation of the mitogen-activated protein kinase Mps1 from the rice blast fungus prevents penetration of host cells but allows activation of plant defense responses. Proceedings of the National Academy of Sciences U.S.A. 95:12713-12718

Table 1. Chemical inhibitors of endocytosis

Chemical	Target	Mode of action	Comments	References
Filipin	CIE*	Binds to sterols in the membrane.	Toxic at higher concentrations.	(Rodal et al., 1999)
Methyl-β-cyclodextrin	CIE	Deplete cellular membranes of sterols by increasing the water solubility of the sterol.	caveolae-dependent endocytosis.	(Rodal et al., 1999)
Chlorpromazine	CME**	Translocates clathrin and AP2 from the cell surface to intracellular endosomes.	Also inhibits CIE in some cells.	(Wang et al., 1993)
Cantharidin	CME	Inhibits PP2A (protein phosphatase 2A)	Affects flg22-mediated FLS2 endocytosis.	(Serrano et al., 2007)
Triclosan	CME	Inhibits PP2A (protein phosphatase 2A)	Affects flg22-mediated FLS2 endocytosis.	(Serrano et al., 2007)
Wortmannin	nd***	Inhibits PI3Ks, blocks late trafficking to the vacuole, multivesicular bodies and endocytosis.	Late endosomes lose their clathrin; Potential CME association.	(Bright et al., 2001; Sachse et al., 2002; Robinson et al., 2008)
Concanamycin A	nd	Targets V-type ATPase and blocks trafficking at trans-Golgi network, endosome acidification.	Induces acidification crucial for endocytic pathways.	(Maranda et al., 2001; Robinson et al., 2008)

*CIE: clathrin-independent endocytosis; **CME: clathrin-mediated endocytosis; ***nd: not determined.

Figure 1

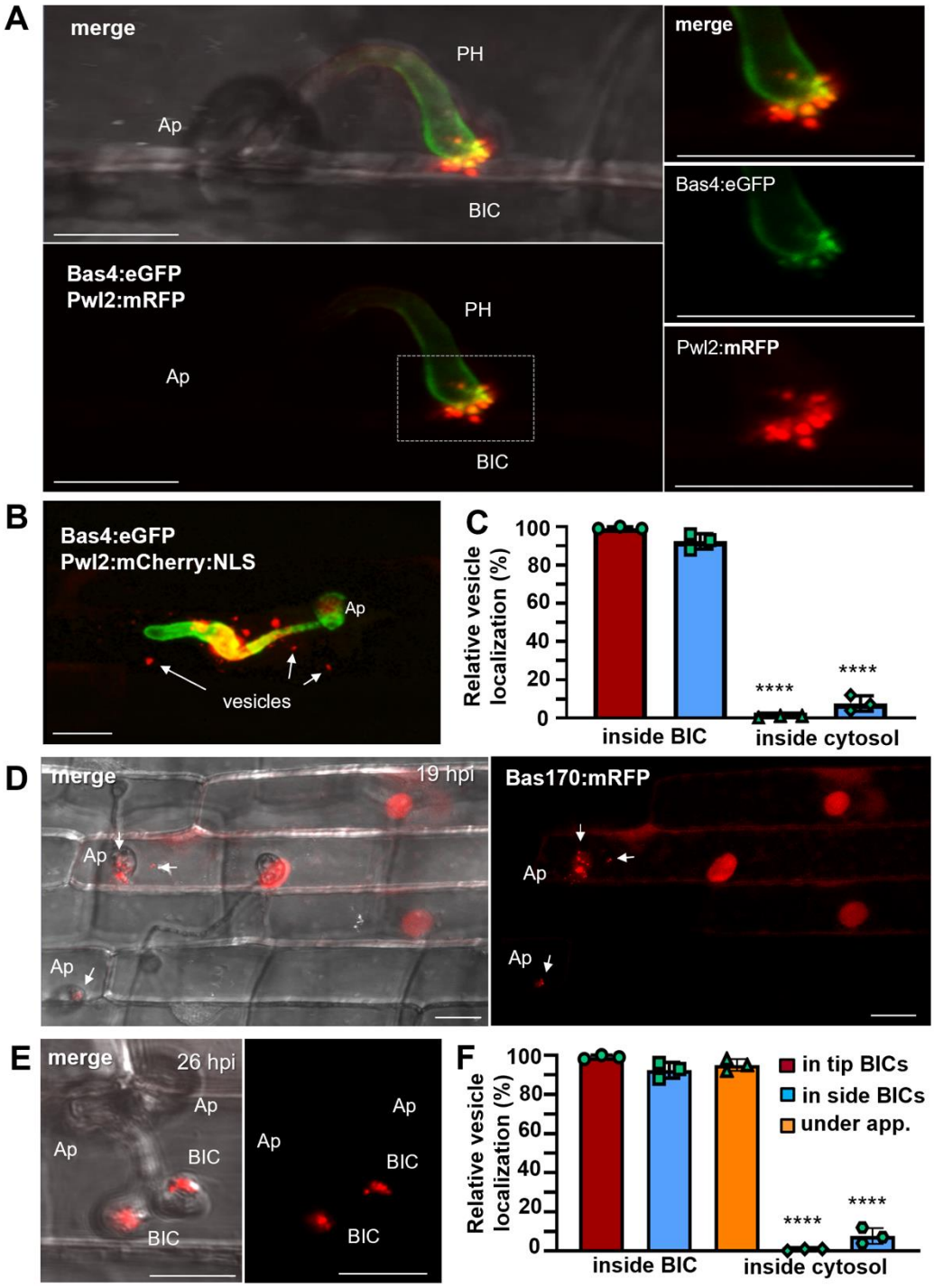

Figure 1. **BIC vesicular organization and effector vesicles in the rice cell cytoplasm**. **A.** Cytoplasmic effector-labeled vesicles in a tip-BIC at the tip of a primary hypha (PH) of strain KV217 expressing Pwl2:mRFP and Bas4:eGFP at 17 hpi. The appressorium (Ap) and the first half of the PH are out of focus. Separate mRFP and eGFP channels (right) for the inset show the base layer of apoplastic effector Bas4:eGFP and the outer vesicular layer labeled by cytoplasmic

effector Pwl2:mRFP. **B.** A side-BIC occurring above a first bulbous IH cell of strain KV168 expressing Pwl2:mCherry:NLS and Bas4:eGFP at 24 hpi. Effector vesicles in are visible in the host cytoplasm at a distance from the BIC. The Bas4:eGFP control shows that the EIHM surrounding the IH remains intact. See additional details in Supplemental Figure S2. **C.** Quantification of the relative localization of cytoplasmic effector vesicles, assessed using strain KV217 from panel A at 98 infection sites for each BIC developmental stage. Bar charts are based on means of three biological reps (data points shown); error bars indicate standard deviation. ****P<0.0001. **D.** Bas170:mRFP, here expressed by *M. oryzae* strain KV224, shows rapid accumulation in vesicles under appressoria and in plant nuclei. At 19 hpi, Bas170:mRFP labels vesicles under appressoria and naturally accumulates in nuclei even before a primary hypha is visible. Arrows indicate vesicles in the rice cytoplasm. Left image shows merged bright field and mRFP fluorescence and right image shows mRFP fluorescence alone. **E.** Bas170:mRFP also localizes to BICs, shown here at 26 hpi in side-BICs resulting from adjacent appressoria penetrating the same rice cell. Experimental details same as in D. **F.** Quantification of the relative localizations of Bas170:mRFP effector vesicles, assessed using data from strain KV224 (D and E) at 98 infection sites for each BIC developmental stage and cytoplasm under appressoria (app.) during fungal penetration. Bar charts with data points from biological replications same as described in C. All images are projections of confocal optical sections. Images in A and B (merged bright field, eGFP and mRFP fluorescence) shown as projections of confocal optical sections. Bars = 10 µm.

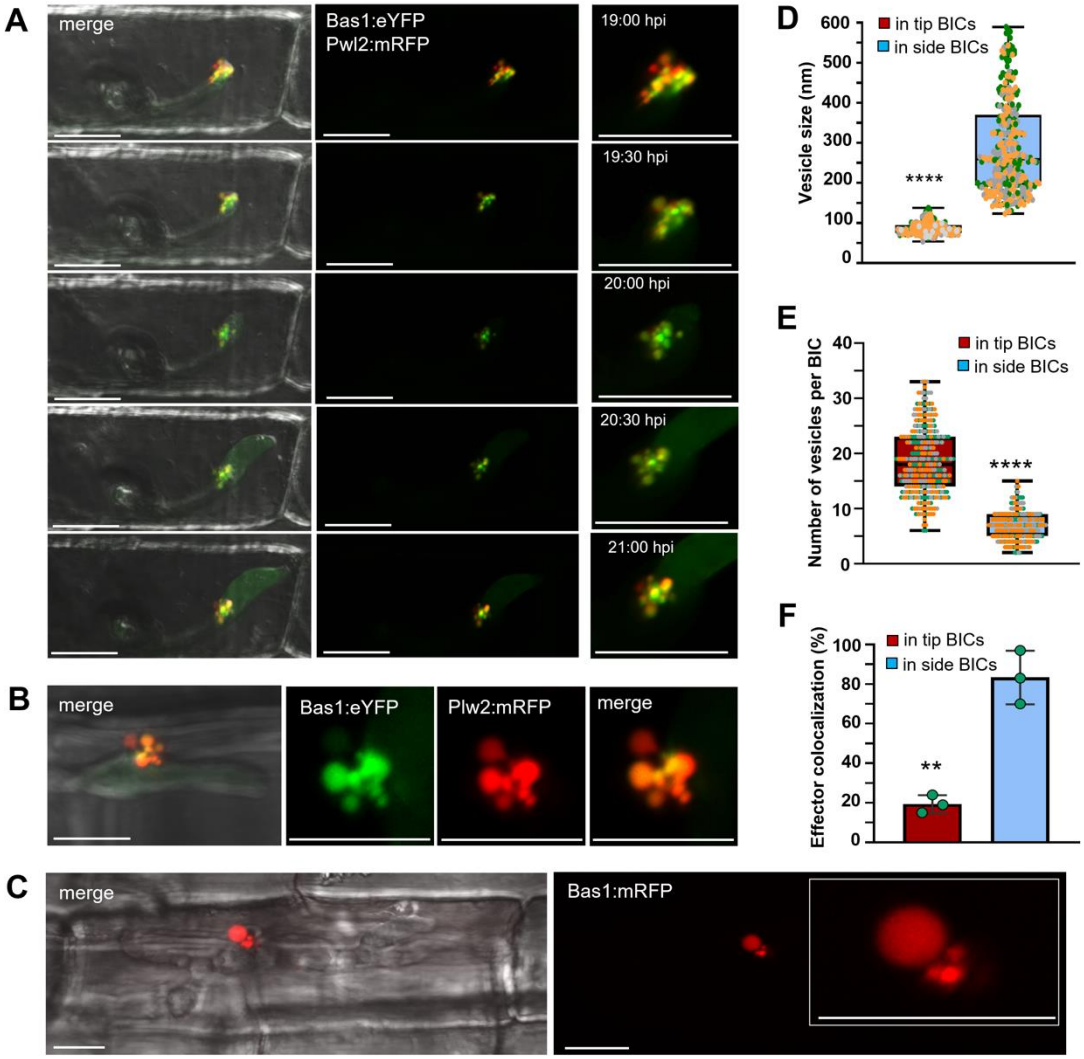

954

955 **Figure 2. Dynamics of BICs and effector vesicles during differentiation of primary hyphae**
956 **to first bulbous invasive hyphae. A.** Dynamics of two cytoplasmic effectors, Pwl2:mRFP and
957 Bas1:eYFP (Strain KV211), as a tip-BIC (top panel) becomes a side-BIC (bottom panel), imaged
958 every 30 min from 19 to 21 hpi. Images (left to right) are merged bright field, eYFP and mRFP
959 fluorescence at 5 time points; merged eYFP and mRFP at same time points in both the same and
960 enlarged views of the fluorescent BICs shown as projections of confocal optical sections. Bars =
961 10 µm. **B.** Cytoplasmic effectors Pwl2:mRFP and Bas1:eYFP (Strain KV211) co-localize in larger
962 vesicles in a side-BIC at 24 hpi. **C.** A rare extremely large effector vesicle (diameter 3.9 µm) in a
963 late stage side-BIC formed by strain KV170 expressing Bas1:mRFP at 30 hpi. **D,E.** Box and
964 whisker plots with individual data points comparing vesicle sizes (D) and number of vesicles (E)
965 in tip- and side-BICs formed by strain KV211 invading rice cells; data points of different colors
966 represent different biological replicates. **F.** Bar chart showing quantification of Bas1:eYFP and
967 Pwl2:mRFP colocalization (KV211) in vesicles in tip- and side-BICs. Bar charts are based on
968 mean values of data points from three biological replicates; error bars indicate standard deviation.
969 **P=0.0015; ****P<0.0001. 100 BICs observed per replicate in D-F.

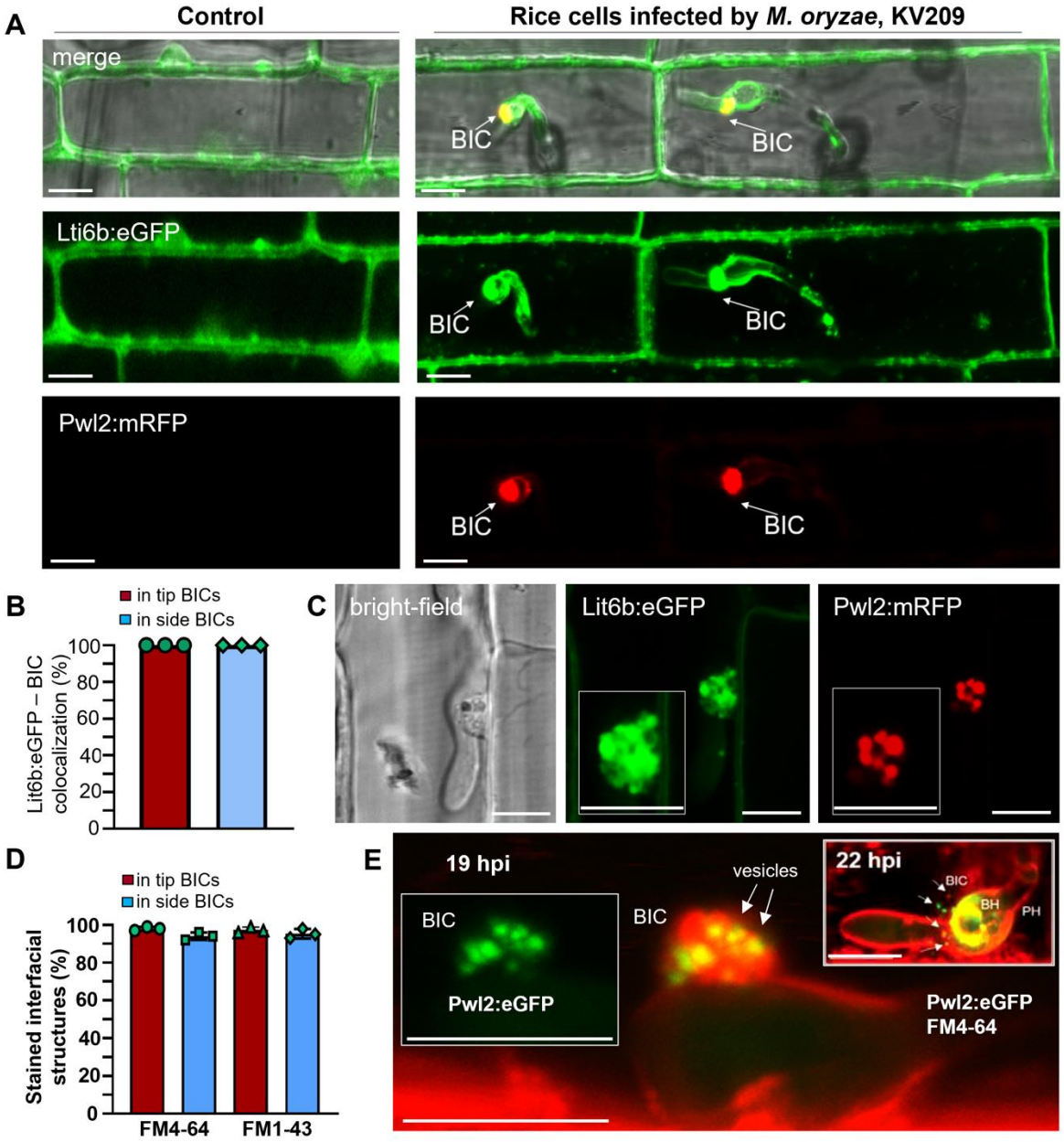

Figure 3. Effector vesicles are derived from plant plasma membrane. A. Rice expressing plasma membrane marker LTi6b:eGFP in non-infected cells (left column) and in cells infected by strain KV209 expressing Pwl2:mRFP (right column). Colocalization confirms BICs as plant plasma membrane-rich structures. **B.** Quantification of the colocalization of LTi6b:eGFP with BICs at both developmental stages. Bar charts are based on means of three biological reps (data points shown); error bars indicate standard deviation; three times 90 infection sites observed. **C.** Localization assays of LTi6b:eGFP relative to Pwl2:mRFP in an infected rice cell at 22 hpi showing LTi6b:eGFP outlining vesicles in the BIC. Insets show BIC vesicles at higher magnification. **D.** Quantification of BICs stained by the endocytosis tracer dyes FM 4-64 and FM 1-43 at the tips of primary hyphae and beside the first bulbous IH. Bar charts are based on means of three biological reps (data points shown); error bars indicate standard deviation; three times 90

infection sites observed per treatment. **E.** Colocalization of BIC effector vesicles and FM4-64-stained membranes in BICs. The main image shows strain KV176 expressing Pwl2:eGFP in a side-BIC in FM 4-64 stained rice at 19 hpi. The image shows merged eGFP and FM 4-64 fluorescence with eGFP fluorescence shown alone in the inset in the lower left. The upper right inset shows a top-down view of a different BIC, shown below the image plane, at 22 hpi. Inset arrows indicate Pwl2:eGFP vesicles near the BIC. Images are projections of confocal optical sections. See Supplemental Movie S2 for yet another side-BIC with additional examples of colocalization of FM 4-64 fluorescence and Pwl2:eGFP. All Bars = 10 µm.

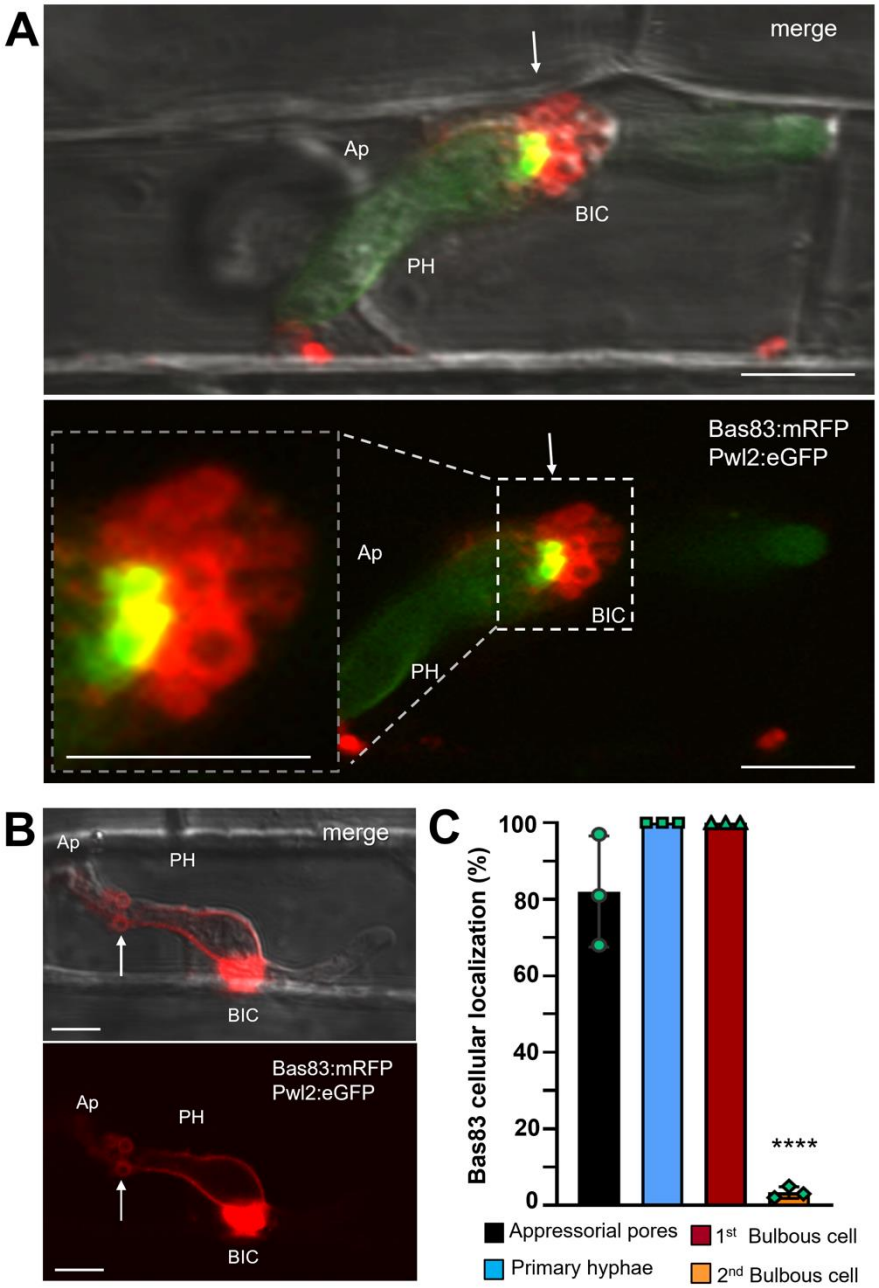

Figure 4. Bas83 is a novel effector associated membrane vesicles surrounding BICs and BIC-associated cells. A. Bas83:mRFP binds apparent membrane vesicles surrounding a side-BIC (white arrow) labeled with Pwl2:eGFP (strain KV222). **B.** Bas83:mRFP (KV220) binds to bubble-like structures near a primary hypha (arrow) as well as labeling a BIC and outlining BIC-associated cells. Images (merged bright field, eGFP and mRFP fluorescence) are projections of confocal optical sections. See additional images in Supplemental Figure S3. Bars = 10 µm. **C.** Quantification of the cellular localization of Bas83:mRFP during biotrophic invasion of *M. oryzae* (KV220). Bar charts are based on means of three biological reps (data points shown); error bars indicate standard deviation. ****P<0.0001; 100 infection sites observed per experiment.

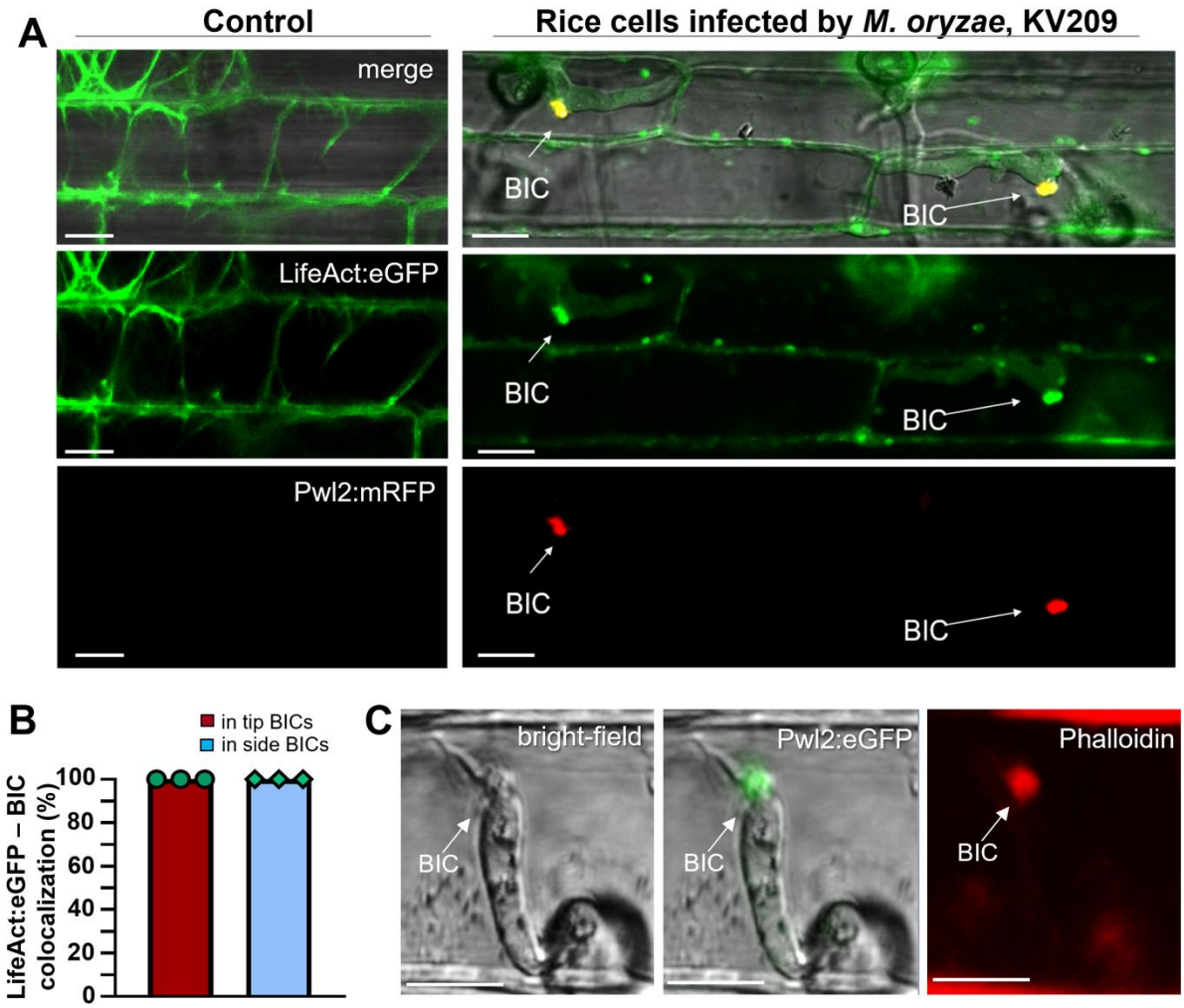

Figure 5. BICs contain plant actin. A. Rice LifeAct:eGFP localization during biotrophic invasion by *M. oryzae*. A rice line expressing LifeAct:eGFP in non-infected cells (left column) and cells infected by *M. oryzae* strain KV209 expressing Pwl2:mRFP in BICs (right column). Colocalization shows BICs are rich in plant actin. **B.** Quantification of the colocalization of LifeAct:eGFP with both tip- and side-BICs. Bar charts are based on means of three biological reps (data points shown); error bars indicate standard deviation; three times 100 infection sites observed. **C.** Rhodamine phalloidin conjugate (red fluorescence staining actin filaments) colocalizes with Pwl2:eGFP in rice cells infected by strain KV176, confirming the actin-rich structure of the BIC.

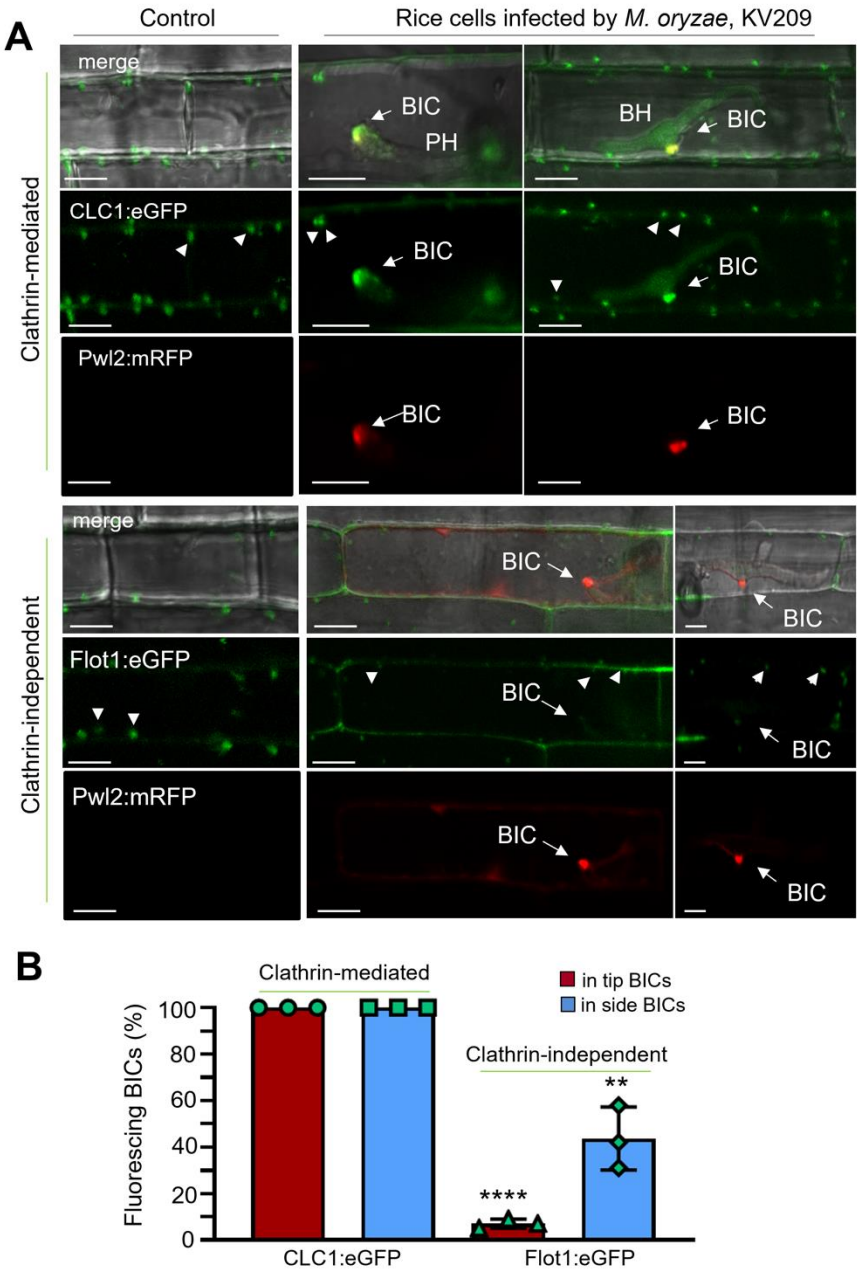

Figure 6. BICs uniformly contain clathrin, but not in flotillin1. A. Rice leaf sheaths expressing OsCLC1:eGFP (top panels) or OsFlot1:eGFP (bottom panels) were inoculated with strain KV209 expressing Pwl2:mRFP. Shown from left to right are a non-infected rice sheath cell; an infected cell containing a primary hypha (PH) with a tip-BIC at 19 hpi; and an infected cell containing a bulbous IH (BH) with a side-BIC at 22 hpi. Arrowheads indicate endocytic foci and arrows indicate BICs. Bars=10µm. **B.** Quantification of the colocalization of OsCLC1:eGFP or OsFlot1:eGFP in both BIC developmental stages. Bar charts are based on means of three biological reps (data points shown); error bars indicate standard deviation; three times 97 BICs observed each treatment. ****P<0.0001; **P=0.002.

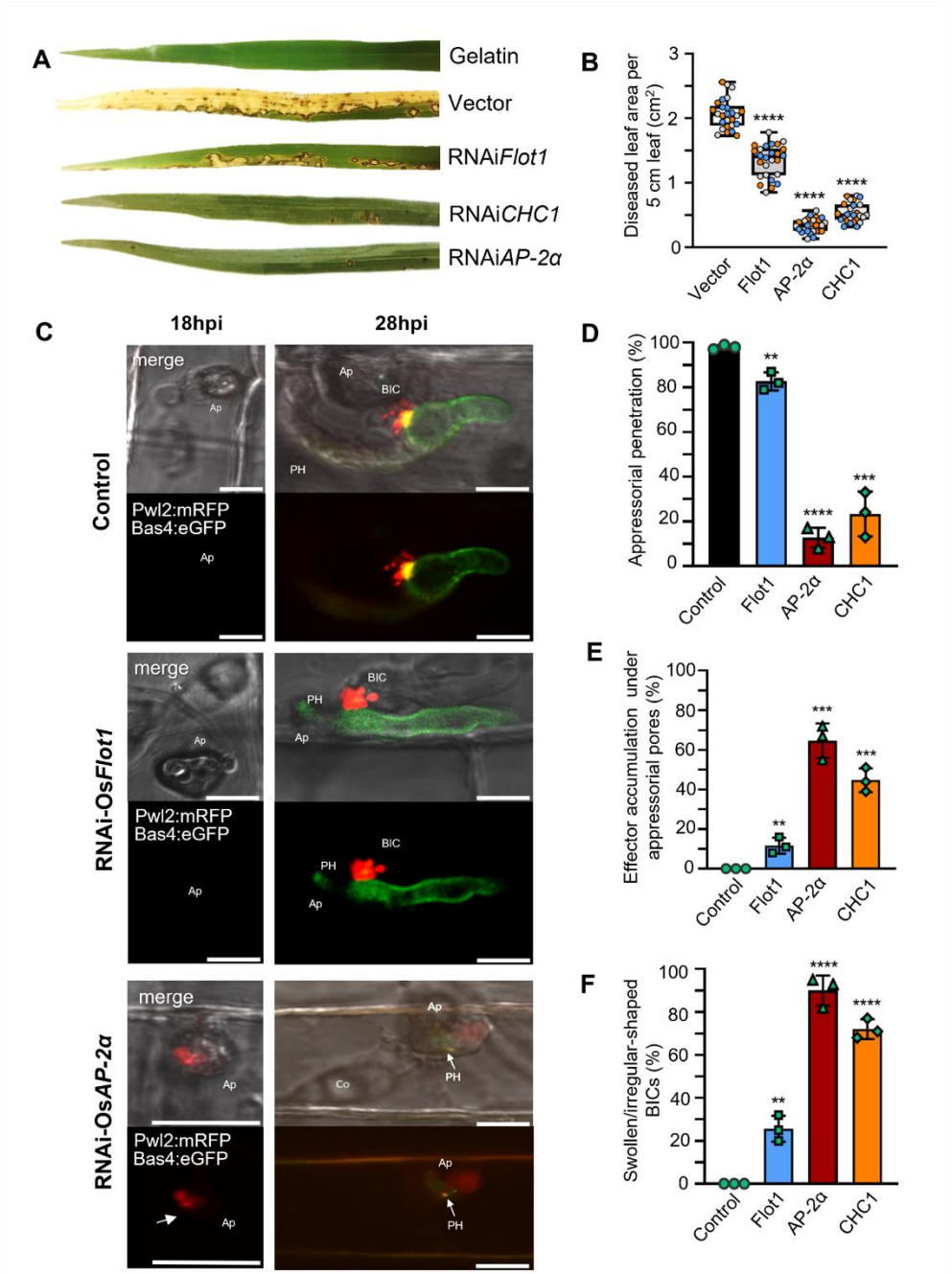

Figure 7. Silencing of rice endocytic machinery suggests roles in pathogenicity and fungal effector translocation. A. Disease severity in rice leaves, cultivar IR64, undergoing silencing of rice endocytic genes**.** Whereas silencing of *Flot1* gene showed minor effects on pathogenesis, the silencing of the key clathrin-mediated endocytosis genes, *AP-2α* and CHC1 resulted in a significant reduction in pathogenicity in whole plant spray inoculation assays. **B.** Quantification of diseased area in 5cm leaf segments in rice expressing RNAi*AP-2α*, RNAi*CHC1*, RNAi*Flot1* or empty vector infected by *M. oryzae* strain Guy11. Box and whisker plots with individual data points are shown; data points of different colors represent different biological replicates. ($P<0.0001$ for all treatments; n = 9 rice plants per replication). **C.** Effects of silencing rice endocytosis genes on the localization of Pwl2:mRFP and Bas4:eGFP during biotrophic invasion.

Wild type IR64 rice and rice expressing RNAi*Flot1* or RNAi*AP-2α* were infected by KV217 expressing Pwl2:mRFP and Bas4:eGFP at 26 hpi. Note the accumulation of Pwl2:mRFP under the appressorium (Ap) and the pale Bas4:eGFP fluorescence associated with the short primary hypha (PH) in the RNAi*AP2α* rice compared to the control and RNAi*Flot1* rice. Images in C (merged bright field, eGFP and mRFP fluorescence) are shown as projections of confocal optical sections. Bars = 10 µm. **D.-F.** Quantification of appressorial penetration (D), effector accumulation under appressoria (E), and swollen irregular BICs (F) in rice expressing RNAi*Flot1*, RNAi*AP-2α*, RNAi*CHC1* or the empty vector during infection by strain KV209 expressing Pwl2:mRFP (~28 hpi). Bar charts are based on means of three biological reps (data points shown); error bars indicate standard deviation. (D: **P=0.0031, ***P=0.0002, ****P<0.0001; E: **P=0.0075, ***P=0.0002; F: **P=0.0018, ****<0.0001; three times 100 infection sites counted per treatment).

Figure 8

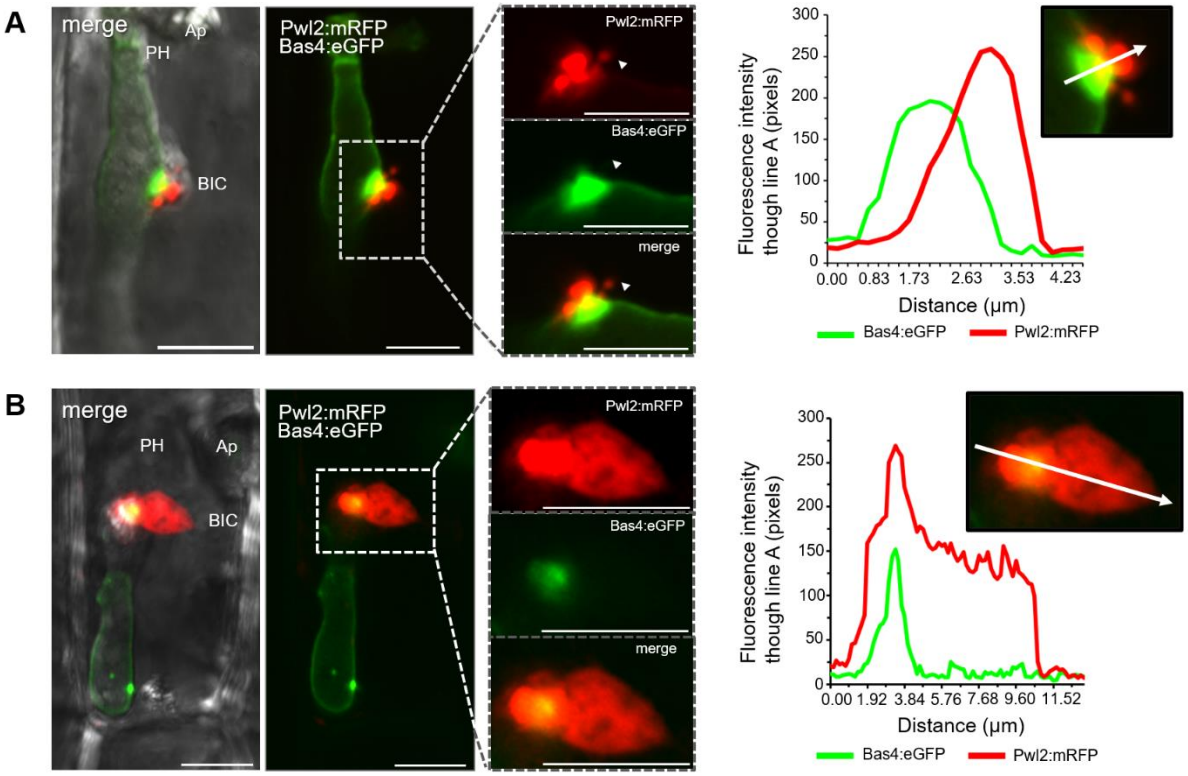

Figure 8. Treatment with CME inhibitor cantharidin impacts the localization of cytoplasmic effector Pwl2, but not apoplastic effector Bas4. A. Apoplastic effector Bas4:eGFP identifies an inner base layer of the BIC relative to cytoplasmic Pwl2:mRFP, as shown by fluorescence intensity linescans for GFP (green) and mRFP (red) along the path of the white arrow. This side-BIC was formed during invasion of rice by strain KV217 expressing Pwl2:mRFP and Bas4:eGFP at 26 hpi. **B.** After treatment with CME inhibitor cantharidin, localization of Bas4:eGFP in the BIC base appears unaffected, compared to the non-vesicular swollen localization of Pwl2:mRFP, as shown by fluorescence intensity linescans for GFP (green) and mRFP (red) along the path of the white arrow. Note linescan distance for Pwl2:mRFP is almost 3-fold greater after cantharidin treatment. This BIC was formed by KV217 at 26 hpi, as in control panel A. Images (merged bright field, eGFP and mRFP fluorescence) are shown as projections of confocal optical sections. Appressorium (Ap); Primary hypha (PH). Bars = 10 µm.

Figure 9

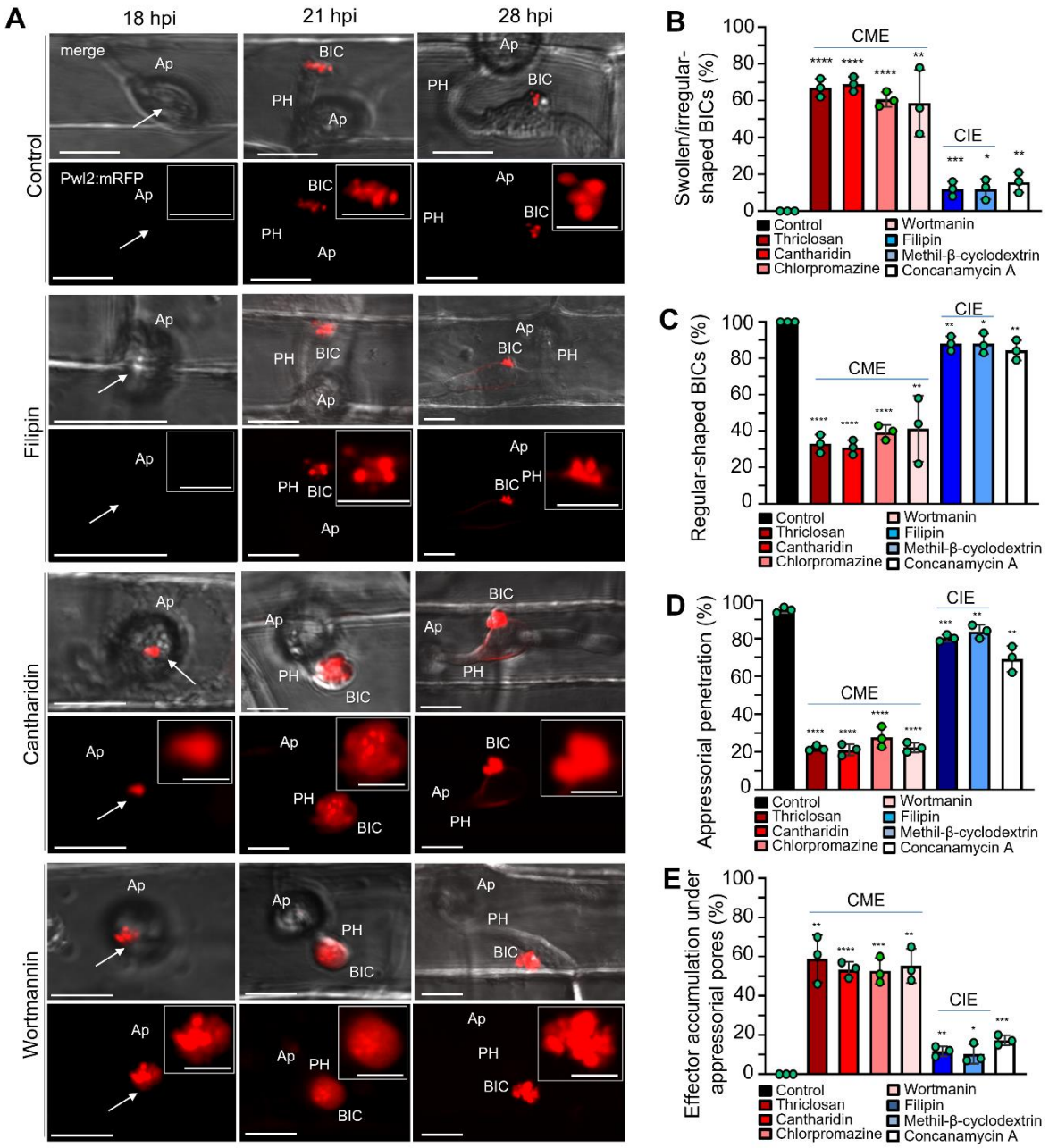

Figure 9. Chemical inhibition of rice CME, but not of CIE, has a major impact on cytoplasmic effector localization and appressorial penetration. A. Effects of chemical inhibition of Clathrin-mediated endocytosis (CME) and Clathrin-independent endocytosis (CIE) in the rice leaf sheath assay with strain KV209 expressing Pwl2:mRFP at 18, 21 and 28 hpi. Whereas inhibition of CIE showed significant, but relatively minor effects on BIC functionality and effector uptake, the chemical inhibition of CME resulted in a significant accumulation of effector fluorescence under appressoria (Ap, white arrows at 18 hpi) as well as swollen BICs on primary hyphae (PH, 21 hpi) and bulbous IH (28hpi). Images in A (merged bright field and mRFP fluorescence) are projections of confocal optical sections. Insets show close-up views of the

effector fluorescence. Bars = 10 µm and bars in the insert boxes = 5 µm. **B-E.** Quantification of swollen, irregular-shaped BICs (B), regular-shaped BICs (C), appressorial penetration (D), and effector accumulation under appressoria (E), in rice undergoing chemical treatment and infection by strain KV209 expressing Pwl2:mRFP at 28 hpi. Bar charts are based on means of three biological reps (data points shown); error bars indicate standard deviation. Three times 100 infection sites observed per treatment. B: *P=0.0202(MβC), **P=0.0065(Filipin), **P=0.0079 (Con.A), **P=0.005(Wort.), ****P<0.0001; C: *P=0.02(MβC), **P=0.0065(Filipin), **P=0.0075(Con.A), **P=0.005(Wort.), ****P<0.0001; D: P=0.0068(MβC), **P=0.0004(Filipin), **P=0.0032 (Con.A), ****P<0.0001; E: *P=0.0222(MβC), **P=0.0013(Filipin), ***P=0.0003(Con.A), **P=0.0004(Wort.), **P=0.0011(Tricl.), ***P=0.0002(Chlorpr.), ****P<0.0001(Canth.).

Figure 10

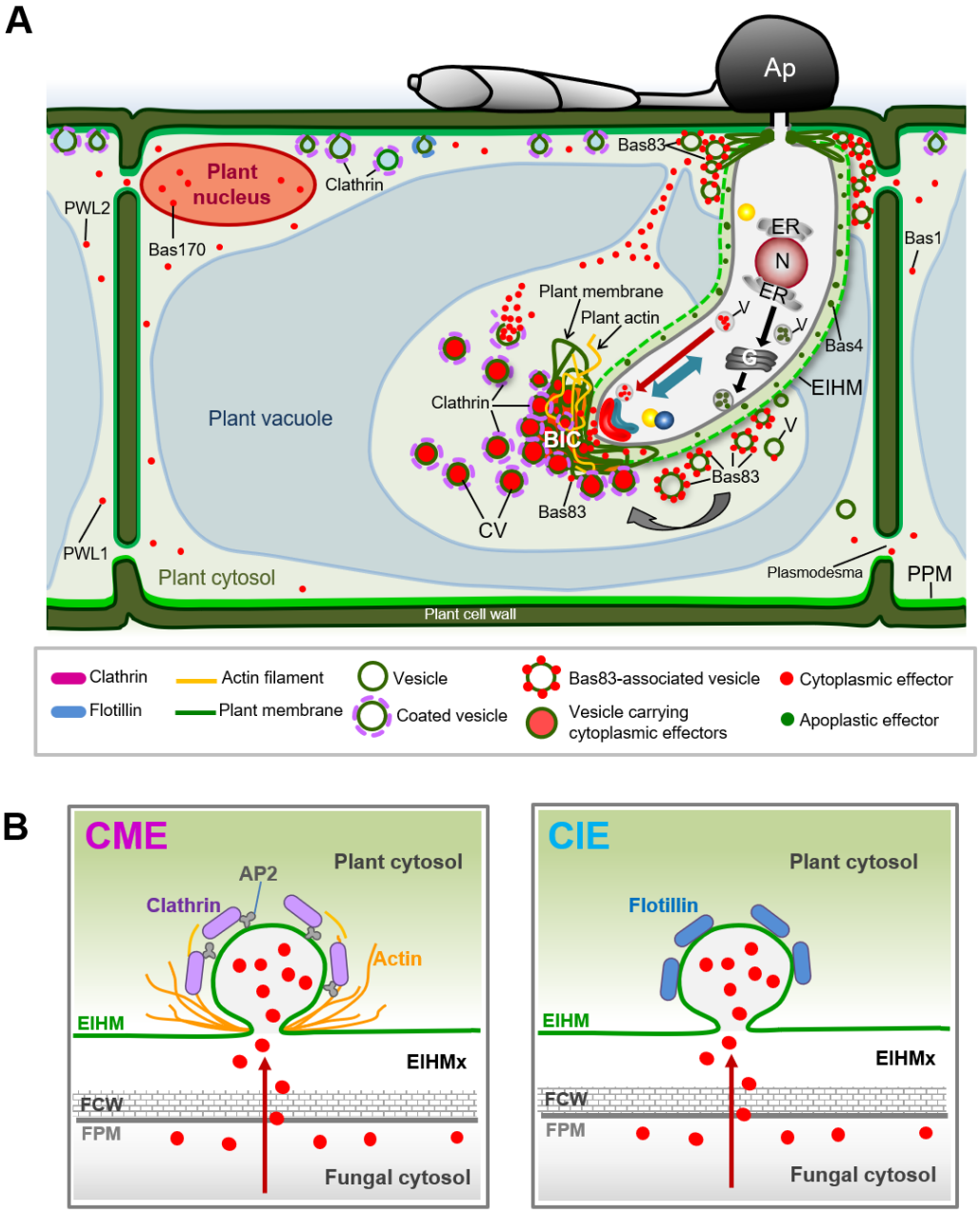

Figure 10. Model for *M. oryzae* effector secretion and translocation into rice cells. A. This cartoon represents the specialized Biotrophic Interfacial Complex at the growing tip of primary hyphae (tip-BIC) at 22–24 h.p.i. (hours post-inoculation), but similar mechanisms apply to side-BICs left behind after differentiation of the first bulbous invasive hyphae (IH). At successful infection sites, apoplastic effectors (dark green circles), including Biotrophy-associated secreted protein-4 (Bas4), are secreted from the PH by conventional golgi-dependent secretion (black arrows), which is blocked by treatment with Brefeldin A. Apoplastic effectors accumulate in the separate compartment enclosed by the EIHM (inside the dark green dashed line around the PH). In contrast, fluorescently-labeled cytoplasmic effectors (red circles), including Pwl2, Pwl1 and

Bas1, are secreted into BICs by a nonconventional, Brefeldin A-insensitive secretion system involving the exocyst and SNARE protein Sso1 (red arrows). Cytoplasmic effectors also accumulate inside the EIHM compartment around the BIC-associated cells, the PH and first differentiated bulbous IH cell (not shown). In contrast, cytoplasmic effectors do not accumulate in the EIHM surrounding nonBIC-associated hyphal cells, which are tightly surrounded by the host vacuole. Our current study expands this model by showing that cytoplasmic effectors are packaged in dynamic vesicles inside BICs and they can sometimes be observed in the host cytoplasm surrounding BICs, and that these effector vesicles co-localize with fluorescent plant plasma membrane markers LTi6B:GFP and FM 4-64, as well as clathrin-mediated endocytosis (CME) marker CLC1:eGFP. These co-localization studies, additional localization with plant actin in BICs, and functional analyses via VIGS and pharmacological inhibitors support CME as a major mechanism for effector translocation. Further research should focus on two novel cytoplasmic effectors we describe. Bas83 labels empty membrane vesicles, possibly recruiting more host membrane to the BIC and the EIHM surrounding BIC-associated cells. Bas170 localizes to effector vesicles directly under the appressorium and accumulates in the host nucleus between BICs and the host cell periphery would facilitate movement of translocated effectors to the host nucleus and other sites of action in the host cell, as well as movement of cytoplasmic effectors through plasmodesmata into surrounding host cells to prepare them for invasion. Key: N, fungal nucleus; ER, endoplasmic reticulum; G, Golgi apparatus; V, transport vesicle. **B.** Working models for vesicle formation and effector translocation in the rice-*M. oryzae* interaction through CME or clathrin-independent endocytosis (CIE). Although our current work supports a role for CME, some involvement of CIE in effector translocation cannot be ruled out as playing a minor role. AP2, Adaptor Protein-2 complex; EIHM, extrainvasive hyphal membrane; EIHMx, extrainvasive hyphal matrix; FPM, fungal plasma membrane; FCW, fungal cell wall.